Exploring Novel Properties of Adenomatous Polyposis Coli: Msi1-Knockout Mice Display Alterations in APC and Intestinal Cell Homeostasis; Topoisomerase IIa Binds to Truncated APC in Human Colon Cancer Cells

By
Amanda Ernlund
B.S., Kansas State University, 2008

Submitted to the graduate degree program in Molecular Biology and the Graduate Faculty of the University of Kansas in partial fulfillment of the requirements for the degree of Master of Arts.

_____
Chairperson – Kristi Neufeld

_____
Yoshiaki Azuma

_____
Liang Xu

Date Defended: 11/30/2011

The Thesis Committee for Amanda Ernlund
certifies that this is the approved version of the following thesis:

Exploring Novel Properties of Adenomatous Polyposis Coli: Msi1-Knockout Mice Display Alterations in APC and Intestinal Cell Homeostasis; Topoisomerase IIa Binds to Truncated APC in Human Colon Cancer Cells

_____
Chairperson – Kristi Neufeld

Date approved: 11/30/2011

Abstract

Colorectal cancer is the second leading cause of cancer-related death in the United States. Adenomatous polyposis coli (APC) is the initiating mutation in 80% of all colorectal cancers. Our lab is focused on understanding functions of APC that promote tumor suppression in the normal intestinal epithelia. As a protein with many functions in the cell, APC is both nuclear and cytoplasmic, with different roles in maintaining cellular homeostasis. In the cytoplasm, APC has been well characterized as a repressor of Wnt signaling, a pathway important in activating proliferation in the intestine. Mutation of APC results in uninhibited Wnt signaling and therefore unrestricted proliferation and expansion of stem cell populations. Though APC has been studied extensively, little is known about how levels of APC are regulated. Recently, our lab showed a double-negative feedback regulatory mechanism between APC and Musashi-1 (MSI1) in cell culture. MSI1 represses translation of APC, while APC, via its role as a negative regulator of Wnt signaling, inhibits transcription of MSI1, a Wnt target gene.

To further understand the role of the APC/MSI1 double-negative feedback loop in intestinal homeostasis, I isolated small and large intestines from mice with germ-line knockout of Msi1 and examined differences in proliferation, differentiation, stem cell populations, and apoptosis in the small intestine. In the large intestine, I examined differences in proliferation, stem cell populations, and apoptosis. I hypothesized that loss of Msi1 in the intestine would cause an increase in APC protein, with a subsequent decrease in Wnt signaling. This decrease in Wnt

signaling would reduce the rate of proliferation, increase differentiation, decrease stem cell populations, and have an effect on apoptosis. I show here that in the small intestines of MSI1 mutant mice, APC protein levels were higher and Wnt target gene levels were lower with loss of Msi1. However, proliferation and differentiation of goblet cells remained unchanged. Stem cell populations were reduced and there was a decrease in apoptosis. In the large intestines of MSI1 mutant mice, APC levels and Wnt target genes were unaffected, while proliferation and stem cell populations were decreased. Based on this evidence, the APC/Msi1 feedback loop may play a role in homeostasis in the small intestine and loss of Msi1 may affect a different signaling pathway in the large intestine, such as Notch.

In the nucleus, APC has been shown to play a role in cell cycle regulation. Our lab showed an interaction between the central portion of the APC protein and topoisomerase IIα, which led to G2 cell cycle arrest. However, whether truncated APC and topo IIα interact in colon cancer cells remained unknown. Here I present data that show that topo IIα interacts with endogenous truncated APC containing previously defined topo IIα binding domains, but not with shorter APC truncations lacking these binding regions.

The studies presented here show that disruption of Msi1 regulation of APC has an effect in the small intestine while Msi1 disruption in the colon has a different effect. Also, longer truncated APC proteins endogenous to colon cancer cell lines interact with topo IIα.

Acknowledgements

I would like to thank my graduate advisor, Dr. Kristi Neufeld, for her dedication to instructing me, her helpful advice, and for providing necessary materials, which allowed me to complete my graduate studies. I would also like to thank fellow graduate students in the lab, Maged Zeineldin and Erick Spears, for providing valuable advice and instruction throughout my graduate studies. Also, undergraduates, Marc Roth, Vinit Nanavaty, and Matt Miller, for assisting with mouse genotyping in the Msi knockout mouse studies. Technician, William McGuinness who provided support for all the projects completed in this thesis. And, my graduate advising committee, Dr. Yoshiaki Azuma and Dr. Liang Xu, who provided beneficial recommendations on my projects.

I would also like to thank the providers of reagents for the work presented here. Dr. Hideyuki Okano provided the Msi1 knockout mice. Dr. Bert Vogelstein provided the HCT116β/w cells used for the Apc/topoisomerase IIα experiments. Constructs for the nuclear localization experiments were provided by Dr. Naoki Watanabe. And, production of the APC-M2 antibody was overseen by Dr. Yoshiaki Azuma.

Funding for the Msi1 knockout project and topo IIα project were provided by NIH Grant Number P20 RR016475 from the K-INBRE Program of the National Center for Research Resources. Additional funding for the Msi1 knockout project included Kansas Masonic Foundation Pilot Research Program, Kansas Masonic Cancer Research Institute, and J.R. and Inez Jay Award, Higuchi Biosciences Center.

Finally, I would like to thank all of the professors and students in the MB department that have helped me throughout my time here at KU.

This work is dedicated to my dad, Scott Ernlund, who has always been supportive of the ventures that I have undertaken. You are greatly missed.

Table of Contents

Chapter 1

Introduction

Colorectal cancer (CRC) is a major contributor to morbidity and mortality especially in the United States where it is the second leading cause of cancer related death in men and women combined. In 2011, it is predicted that nearly 150,000 individuals will develop CRC and 50,000 will die from this malignancy. One in twenty individuals are at risk for developing CRC in their lifetime (American Cancer Society(66)). World-wide an estimated 1.2 million new cases of CRC are diagnosed (*1*).

Contributing factors of CRC include both lifestyle choices as well as genetic factors. Lifestyle choices that contribute to CRC include heavy drinking, smoking, obesity, and highly processed meat and red meat intake as well as a sedentary lifestyle (*2*). However, many people acquire CRC who do not meet these criteria (*3*). Also, inflammatory bowel disease, including Crohn's and ulcerative colitis, play a key role in CRC with one third of CRC incidence due to chronic inflammatory diseases (*4*). Genetic predisposition also plays a large role in contributing to risk of acquiring CRC. About a quarter of people with family members that have CRC have a higher risk than the general population to develop CRC (*5*). An estimated 30% of CRCs are inherited and 5% of these are attributed to well-characterized syndromes (*6*). These syndromes include hereditary nonpolyposis colorectal cancer (HNPCC), which constitutes a significant portion of inherited cases and is due to mutation of mismatch repair genes. A smaller portion can be attributed to familial adenomatous polyposis (FAP), which results in the patient having hundreds to thousands of colonic polyps in young adulthood and ultimately colon cancer by middle age (*6*).

FAP is due to germ-line mutation of tumor suppressor *Adenomatous polyposis coli* (*APC*).

The specific genetic defects that lead to the progression of CRC have been well-characterized and correlate with the morphological staging of the disease (*7*). Underlying the initiation of CRC is formation of a benign adenomatous polyp, which is caused by mutation of both alleles of *APC*. This mutation is usually followed by mutation of K-Ras or B-raf. CRC precursors are genetically unstable, typically possessing chromosomal instability (CIN) or microsatellite instability (MSI) which are mutually exclusive pathways that lead to acquisition of genetic mutations (*8*). CIN is most often encountered with FAP and a majority of sporadic CRCs. In about 15% of CRCs where mismatch repair (MMR) genes are inactivated, MSI is the mechanism for further genetic mutation(*3*). In either case, genetic instability ultimately leads to inactivation of p53 and carcinoma.

Architecture of the intestinal epithelium

The adult intestinal mucosa is composed of a single epithelial sheet, which works to absorb water and nutrients and secrete protective substances into the lumen of the intestine. The small intestinal epithelium lines the two structural units of the small intestine: the villi, which protrude from the luminal surface, and crypts, which invaginate into the submucosa. The epithelia is composed of a differentiated cell population including: enterocytes which absorb nutrients and water from the intestine, the goblet cells which secrete a protective layer of mucus and enteroendocrine cells which stimulate secretion of specific digestive enzymes.

Paneth cells, a fourth differentiated cell type, secrete antimicrobials and can be found in the crypt base of the small intestine. Villi contain the differentiated cells from multiple crypts. In the large intestine, which lacks villi, the differentiated cells are located on the smooth luminal surface. The differentiated cells of the large intestine include absorptive colonocytes and mucus secreting goblet cells(*9*).

Proliferation in the intestine moves upward along the axis of the crypt to the luminal surface of the intestine. Proliferating cells can be found in the bottom 2/3 of the crypt whereas the differentiated cells are found along the top 1/3 of the crypt as well as in the villi. The cells at the crypt base are comprised of stem cells as well as Paneth cells. The stem cells divide to give rise to transit amplifying cells, which move up the crypt axis and further divide. Once the transit amplifying cells reach the crypt-villus axis, they differentiate to become the functional cells of the intestine. The exception to this upward movement of differentiated cells are Paneth cells which move to the base of the crypt (*10*). The differentiated cells are short-lived and undergo apoptosis and are shed into the lumen or engulfed by neighboring cells or macrophages (*11*). This process of cell turnover in the intestine can take anywhere from 3 days(*12*) to 5 days(*10*) in mice. Because of the high turnover rate of the intestine, maintenance of intestinal homeostasis is essential so as to avoid carcinogenesis (for overview of intestinal homeostasis see fig. 1.1).

Underlying the intestinal mucosa is the lamina propria containing various cell types. One of these cell types, the intestinal fibroblast, constitutes the stem cell niche along with basement membrane around the area of the stem cells and other extracellular components (*13*). The myofibroblasts concentrate around the crypt

and secrete signals that allow for epithelial proliferation and differentiation (*14*). These signals are predominantly from the Wnt, Notch, BMP, and Hedgehog pathway. Below, I will briefly review the roles of Wnt and Notch in intestinal stem cell maintenance. Review of the BMP and Hedgehog pathways can be found in (*10*)

Along with being critical for intestinal stem cell maintenance, Wnt signaling is critical for the maintenance of the whole intestinal epithelium(*7, 15, 16*) and disruption of Wnt signaling is an initiating event to drive the transformation of normal intestinal mucosa to adenocarcinoma (*7*). The Wnt signaling pathway is mediated by phosphorylation events of β-catenin as determined by presence or absence of a Wnt signal. When the Wnt signal is absent, a destruction complex composed of tumor suppressor adenomatous polyposis coli (APC) and axin will bind to B-catenin and two other destruction complex proteins, GSK3 and CK1 will phosphorylate B-catenin. Phosphorylation of B-catenin recruits the E3 ubiquitin ligase, βTrCP, which will ubiquitinate B-catenin, leading to its eventual degradation by the proteosome. When the Wnt signal binds to its cognate receptor which includes a protein from the Frizzled family as well as Lrp5/6, the destruction complex is inhibited from binding B-catenin by as yet unknown mechanisms. B-catenin will then translocate into the nucleus where it will activate transcription cofactors Tcf and Lef and Wnt target genes will be expressed (*17*). For overview of the Wnt pathway refer to fig. 1.2. There are approximately 50 known Wnt target genes (Standford.edu Wnt Homepage(65)). Normal Wnt signaling allows for proliferation and turnover of stem-cell populations whereas aberrant Wnt signaling allows for continual uncontrolled renewal of stem cells (*17*).

Along with Wnt signaling, Notch signaling has been implicated in maintaining the undifferentiated and proliferative state in the intestine. Notch also helps to determine cell fate decisions in the intestine by specifically controlling cell fate choices between neighboring precursor cells. Notch encodes a transmembrane receptor that is proteolytically cleaved following binding to ligand expressed by a neighboring cell. This cleavage event is followed by subsequent translocation of the Notch intracellular domain (NCID) into the nucleus. The NCID binds a transcriptional repressor, CSL, causing it to become an activator of Notch target genes. The best known Notch target genes encode Hes protein which acts as a transcriptional repressor (*10*).

Notch signaling in the intestine has been implicated in the decision between enterocyte and secretory cell lineages in early progenitor cells (*18-20*). Upon inhibition of Notch signaling via gamma-secretase inhibitors or CSL removal, proliferative cells were converted into goblet cells(*18*). Additionally, overexpression of the Notch1 receptor in all epithelial intestinal cells caused an increase in proliferation and an inhibition of secretory lineages including Paneth, Goblet, and enteroendocrine cells(*19, 20*).

Notch signaling also works synergistically with Wnt signaling to activate proliferation in progenitor populations. Notch1 was found to be expressed in both stem-cell subpopulations in the crypt as well as in transit-amplifying cells (*19*). And, Wnt signaling has been implicated to activate Notch signaling by β-catenin transcriptional activation of Notch ligand in colorectal cancer cells (*21*). Also, activation of Notch signaling is found to inhibit apoptosis (*22*). Finally, Msi1

overexpression enhances proliferation in progenitor populations (*23*). Therefore Wnt and Notch act synergistically to promote proliferation in the progenitor compartment of the intestine and to promote colorectal cancer.

Intestinal Stem cells

Cancer initiating mutations are proposed to originate in the stem cell because these cells have the capacity for longevity required to obtain the necessary number of mutations that lead to cancer(*24*). Stem cells are defined as having four characteristics: they are undifferentiated, can give rise to all cell types of the intestine, can regenerate when damaged, and can give rise to new stem cells over a long period of time (*10*). There have been two populations of stem cells identified in the small intestine that meet these criteria(*25*). The slow cycling stem cell population is marked by Bmi1(*26*). These cells are located at +4 position in the crypt and estimates of stem cells in the +4 position range from 4-6 cells which can be killed by small doses of radiation(*12, 27*) The other stem cell population is composed of crypt-based columnar cells marked by Lgr5 and located between paneth cells. These cells, unlike Bmi1+, cells are actively cycling and undergo apoptosis only with high dosages of radiation (*28*). In two separate mouse models, one with conditional loss of APC and the other with an activating mutation in β-catenin, both populations of stem cells were shown to initiate adenoma formation (*29, 30*). Therefore, the adenoma-initiating cells appear to be stem cells and maintenance of "stemness" in these adenomas leads to initiation of tumors.

Musashi1 has also been shown as a putative stem cell marker, labeling both Lgr+ and Bmi1+ stem cell populations(*31, 32*). In support of its role in stem cells, Msi1 + cells were seen to increase in the stem cell compartment of the crypt following irradiation. However, using immunohistochemistry, Potten et al, also showed that Msi1 potentially labels cells above the stem cell region of the crypt and thereby may also label some transit amplifying cells (*31*).

Musashi-1

Musashi-1 (Msi1) is an RNA-binding protein composed of 362 amino acids and with a molecular weight of approximately 39kDa in mice (*33*). Msi1 was first discovered to be important for development of adult external sensory organs in Drosophila, a model system that has been effectively used to understand mechanisms that control asymmetric cell division in development. Specifically, Msi1 was found to be important for asymmetric divisions of sensory organ precursor cells (*34*). Msi1 was also found to be active in mitotic cell populations in neuronal and glial precursor cells as well as neural stem cells during neurogenesis in mice as well as in ovaries and the small intestine of mice(*33*).

Msi1 acts as a translational repressor by binding to the 3'UTR of target RNA and competing with PABP interaction with eIF4a, thus inhibiting formation of the 80S ribosome complex (*35*). Msi1 is key in maintaining cells in an undifferentiated state, thereby allowing for cell fate decisions to occur (*22*). Key targets of Msi1 translational inhibition include *m-numb* an inhibitor of the Notch pathway. Msi1 was therefore found to be an activator of the Notch pathway, leading to self-renewal

of neural stem cells as well as a non-differentiated state(*22*). Msi1 was also found to be a translational inhibitor of $p21^{WAF-1,}$ a cyclin-dependent kinase inhibitor. Upon overexpression of Msi1 in HEK293 cells and P19 neuronal differentiating cells, proliferation was found to increase as well as an increase in the number of actively cycling cells. Loss of Msi1 caused a premature exit from the cell cycle in neural development (*36*). In both numb and $p21^{WAF-1}$ translational repression by Msi1, mRNA levels were not found to be affected (*22, 36*).

Msi1 expression has been correlated with CRC as a driving force for tumorigenesis and as a marker of metastatic cancer. Msi1 mRNA was found to be higher in human colorectal adenocarcinoma than in surrounding normal mucosa (*31, 37*). Also, Msi1 expression is increased in $APC^{Min/+}$ mice tumors compared with normal tissue (*31*). $APC^{Min/+}$ mice carry a truncating mutation in APC and are commonly used as a model for colorectal cancer. In a mouse xenograft model, siRNA-mediated knockdown of Msi1 led to inhibition of tumor growth, reduced proliferation of cancer cells, and increased apoptosis both alone and with radiation. Also, Msi1 knock down in HCT116 cells, a colon cancer cell line, resulted in increased $p21^{WAF-1}$ protein levels and cell cycle arrest. Notch signaling was found to decrease, allowing for a subsequent increase in mitosis (*37*). Finally, Msi1 levels were found to be an important prognostic indicator in patients with colorectal cancer both in the primary tumor and as an indicator of metastatic spread(*38*).

APC

Familial adenomatous polyposis (FAP) is an autosomal dominant disorder where patients develop colorectal cancer. Patients with FAP usually acquire colonic adenomas as early as their teenage years and by age 40 or 50 these patients will have colorectal cancer. As treatment for this disorder, patients undergo removal of the colon to ensure that the hundreds to thousands of polyps present in the colon do not give rise to cancer(*39*).

Germ-line mutation of *APC* was first linked to FAP . A deletion of 5q21 was linked to patients with FAP (*40*). The gene was cloned and the *APC* mutation was shown to be heterozygous in the colon of FAP patients though the mechanism for initiation of polyps was still unknown (*41, 42*). In support of Knudson's two-hit model of inactivation of tumor suppressor genes, Ichii et al. and Levy et al. determined that loss of heterozygosity or mutation of the other wild-type *APC* allele allowed for early tumorigenesis events to occur(*43, 44*). The *APC* mutations in sporadic colorectal cancer have been found to be identical to those found in FAP(*45*).

APC has been shown to be expressed ubiquitously throughout the body (*42*) and also is important in development. APC is predominantly expressed at the basolateral membrane in the intestine, and it's expression increases in a gradient that moves up the length of the crypt (*46*). Germ-line mutation or knockout of APC is embryonic lethal, causing improper anterior-ventral morphogenesis in the embryo (Ishikawa, 2003; Moser, 1995). Also, conditional knockout of APC in adult mice leads to disruption of proliferation patterns in the small intestine as well as abnormal differentiation of small intestinal cells (*15*). Though APC is necessary for

development, it is not lost as an initiating step in other cancers. APC is therefore considered a gate-keeping gene in the intestine, providing a pivotal role in regulation of intestinal homeostasis(*45*).

APC is a multi-domain protein that interacts with a number of binding partners and performs the role of a scaffold protein in Wnt signaling. It's 2,843 amino acids in size and 312 kDa (*47*). The N-terminal region of the protein is necessary for homodimerization, and in colon cancers, full-length APC can dimerize with mutant forms of APC (*48*). The armadillo region of the protein has been shown to be important for binding to PP2A and ASEF-2(*49, 50*). The 15-amino acid region and 20 amino acid region have been shown to be important for β-catenin binding(*51-53*), though the 20 amino acid region is necessary for β-catenin downregulation (*51*). The SAMP repeats located between 20 amino acid repeats are necessary for APC binding to axin, another scaffold protein in the destruction complex (*54*). For a diagram of the APC protein, refer to fig. 1.3.

Somatic mutations of *APC* that occur in colon cancer appear in the mutation cluster region whereas germ-line mutations of *APC* are found throughout the 5'end of the gene. These mutations are typically nonsense or framshift mutations that result in the truncation of the C-terminal half of the protein(*55*). Mutations disrupt the ability of APC to bind to β-catenin and therefore β-catenin accumulates in the nucleus and control of Wnt signaling is lost.

APC, a predominantly cytoplasmic protein, has been shown to have a nuclear role as well that may allow for distinction of actively proliferating cells (*56*). APC has been shown to contain 2 classic nuclear localization signals as well as 5 nuclear

export signals that allow for it to shuttle between the nucleus and the cytoplasm(*57-59*). Full-length APC appears in both the nucleus and cytoplasm in normal human colonic crypts. In human polyps and carcinoma, full-length APC is found predominantly in the cytoplasm while truncated APC is found in both nucleus and cytoplasm (*60*). The function of APC in the nucleus has been thought to include further regulation of β-catenin via sequestration of β-catenin from TCF/Lef, interaction with repression machinery that competes with TCF/Lef for activation of Wnt target genes, and facilitation of nuclear export of β-catenin(*56*). APC has also been shown to have a potential role in DNA repair through interaction with binding partners polymerase B and PCNA(*61*). Another potential role of APC is in cell cycle regulation via its interaction with topoisomerase IIα (*62, 63*).

Msi1 and APC

Our lab recently demonstrated a double-negative feedback loop between Msi1 and APC (*64*). In cell culture, overexpression of Msi1, a translational inhibitor, was shown to inhibit translation of mRNA containing the APC 3'UTR while loss of Msi1 showed an increase in APC protein levels. Loss of APC lead to an increase in Msi1 protein and mRNA. These findings lead to a predicted model of Msi1 being a direct inhibitor of APC translation (*64*). Msi1 was also found to be a Wnt target gene (*23*).Therefore, APC via inhibition of the Wnt pathway, is an inhibitor of Msi1 transcription and translation.

In the next chapter of this dissertation, we investigated the role of Apc/Msi1 double-negative feedback regulation in the intestines of $Msi^{-/-}$ mice, a mouse model with germ-line knockout of Msi1. To determine whether loss of Msi1

affected Apc, Apc protein levels were examined and found to be higher in the small intestine and unchanged in the large intestine compared to $Msi^{+/+}$ mice. Wnt target gene levels were assessed and were shown to be downregulated in the small intestine and unchanged in the large intestine. These results lead to a hypothesis that the double-negative feedback loop was possibly more prevalent in the small intestine. Next, different phenotypes related to Wnt signaling were examined. In the small intestine, proliferation as scored by Ki-67 immunohistochemistry was examined and no difference was found. Also, differentiation of goblet cells as examined by alcian blue staining yielded no difference between the two genotypes. However, crypt fission was found to be elevated while crypt protrusion growth was found to decrease. And, apoptosis was found to be decreased. In the large intestine, proliferation, as scored by Ki-67, was found to decrease. Crypt fission was found to be decreased and no effect on apoptosis was observed. Together, these results illustrate that the double-negative feedback regulation between Apc and Msi1 may be more prominent in the small intestine and loss of Msi1 in the colon may be affecting more than just this particular regulatory mechanism.

Summary

Colorectal cancer is a significant disease with a large impact on the U.S. population. Colorectal cancer results from multiple mutations in tumor suppressors and oncogenes that lead to the loss of homeostasis in the intestinal epithelium, disrupting the natural process of proliferation, differentiation, and apoptosis. These mutations are proposed to arise in the stem cells that govern cell turnover in the

intestine because these cells have a long life span, which would allow for accumulation of mutations. Msi1, a purported marker of stem cells, allows cells to remain in an undifferentiated and proliferative state through its inhibition of inhibitors of cell cycle progression and Notch signaling. Msi1 was also shown to regulate APC via inhibition of its translation. *APC* is mutated in 80% of all CRCs as the initiating step in tumorigenesis. *APC* mutation allows for uncontrolled Wnt signaling in the intestine. Msi1, a Wnt target, is thereby influenced by *APC* mutation and is therefore produced at higher levels. This disruption of regulation between APC and Msi1 would allow for uncontrolled levels of Msi1 protein and thereby a mechanism for cells to remain in a stem-like state. Msi1 could thereby be an attractive target for therapy.

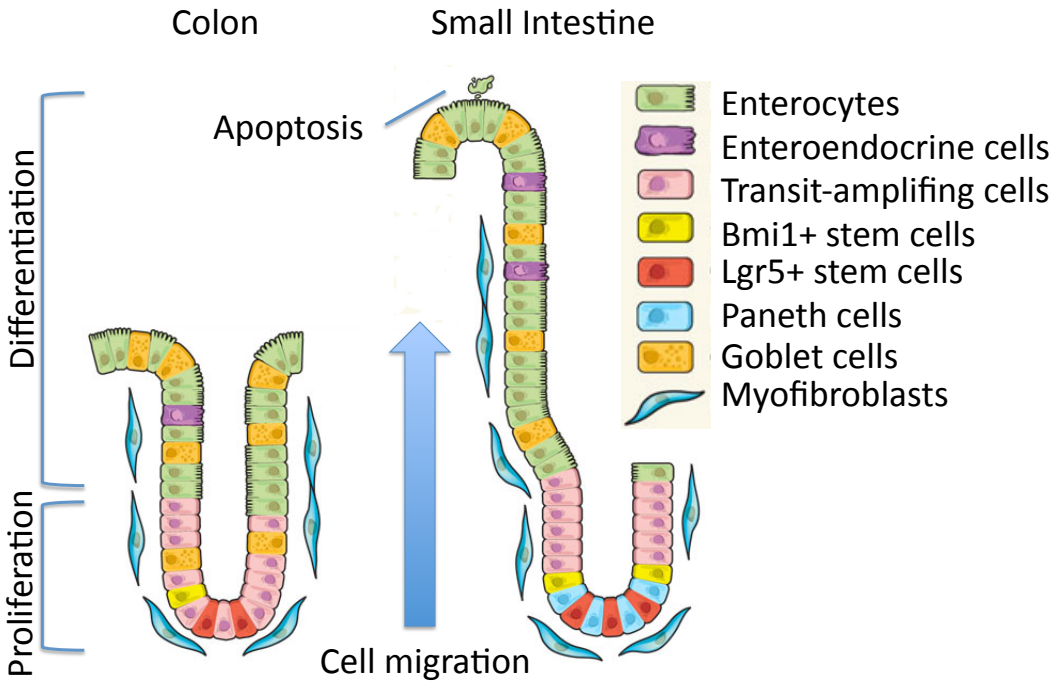

Figure 1.1. ***Intestinal Homeostasis.*** **Cells in both the large and small intestine migrate from the base of the crypt where stem cell populations exist, towards the lumen of the intestine where they undergo apoptosis and are shed in a few days. As they move upwards and leave the proliferative progenitor compartment, they differentiate into goblet, enteroendocrine, and enteroendocrine cells, or their respective counterparts in the colon. Paneth cells, a fourth type of differentiated cell in the small intestine, moves to the crypt base. Adapted from Medema, J. P. and Vermeulen, L. (2011).** ***Nature,*** **474 (7351), 318-26.**

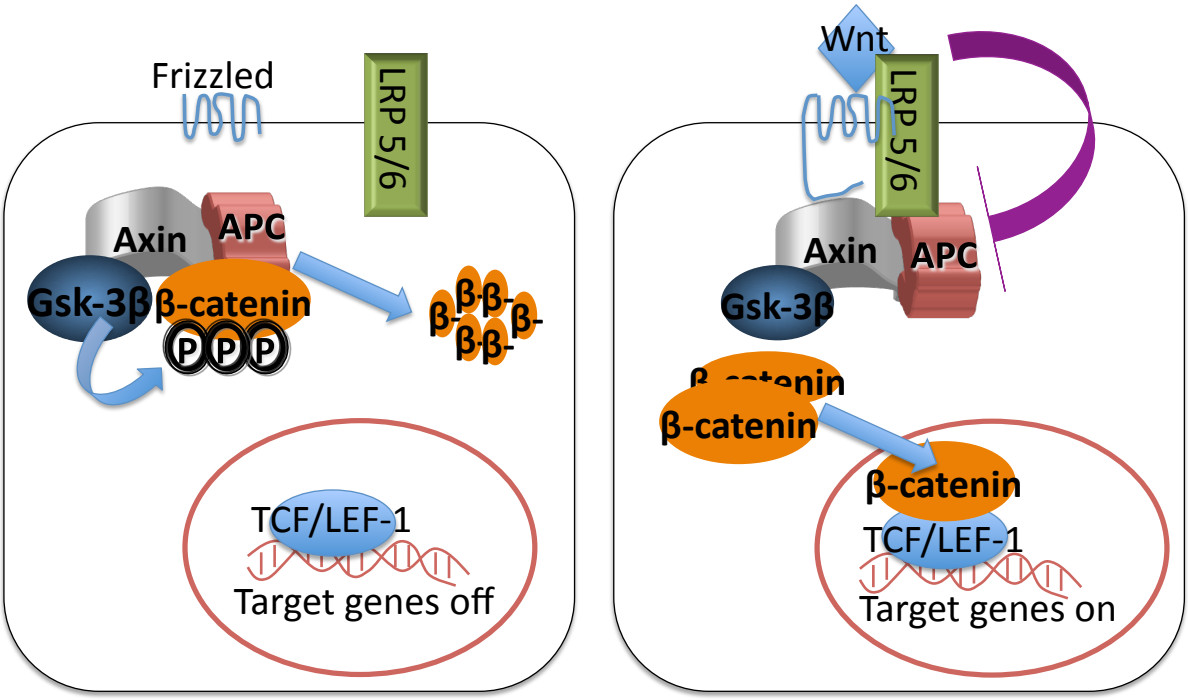

Figure 1.2. ***Wnt signaling in the intestine.*** **In the left panel, when the Wnt signal is absent, the destruction complex composed of APC, Axin, and Gsk-3β will bind β-catenin and Gsk-3β will phosphorylate it. Phosphorylation of β-catenin leads to recruitment of βTrCP (not pictured) which ubitquitinates β-catenin leading to proteosomal degradation. In the right panel, when the Wnt signal is present, the destruction complex is inhibited by mechanisms unknown and β-catenin translocates into the nucleus. β-catenin will then bind TCF/LEF-1 transcription factors, which will allow for transcription of Wnt target genes.**

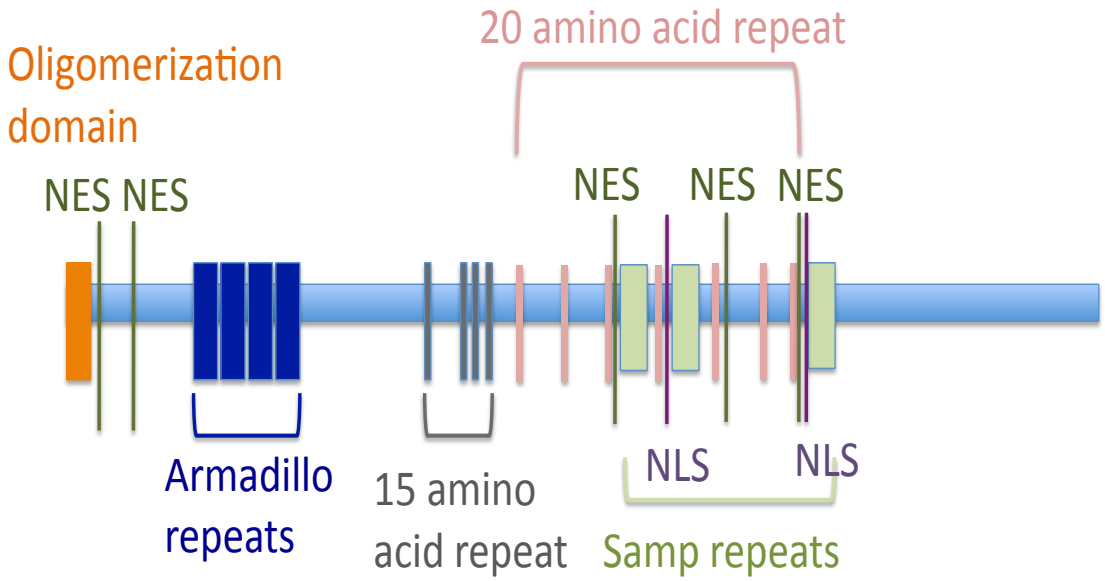

Figure 1.3. ***Domains of APC.*** **APC is a multi-domain protein with many cellular functions. Depicted here is the full-length protein with some of the different domains, nuclear export, and localization signals represented.**

References

1. Ferlay, J., Shin, H. R., Bray, F., Forman, D., Mathers, C., and Parkin, D. M. (2010) Estimates of worldwide burden of cancer in 2008: GLOBOCAN 2008, Int J Cancer 127, 2893-2917.
2. Huxley, R. R., Ansary-Moghaddam, A., Clifton, P., Czernichow, S., Parr, C. L., and Woodward, M. (2009) The impact of dietary and lifestyle risk factors on risk of colorectal cancer: a quantitative overview of the epidemiological evidence, Int J Cancer 125, 171-180.
3. Fearon, E. R. (2011) Molecular genetics of colorectal cancer, Annu Rev Pathol 6, 479-507.
4. Cunningham, D., Atkin, W., Lenz, H. J., Lynch, H. T., Minsky, B., Nordlinger, B., and Starling, N. (2010) Colorectal cancer, Lancet 375, 1030-1047.
5. Kerber, R. A., Neklason, D. W., Samowitz, W. S., and Burt, R. W. (2005) Frequency of familial colon cancer and hereditary nonpolyposis colorectal cancer (Lynch syndrome) in a large population database, Fam Cancer 4, 239-244.
6. Jasperson, K. W., Tuohy, T. M., Neklason, D. W., and Burt, R. W. (2010) Hereditary and familial colon cancer, Gastroenterology 138, 2044-2058.
7. Fearon, E. R., and Vogelstein, B. (1990) A genetic model for colorectal tumorigenesis, Cell 61, 759-767.
8. Jass, J. R. (2007) Classification of colorectal cancer based on correlation of clinical, morphological and molecular features, Histopathology 50, 113-130.
9. Radtke, F., and Clevers, H. (2005) Self-renewal and cancer of the gut: two sides of a coin, Science 307, 1904-1909.
10. Sancho, E., Batlle, E., and Clevers, H. (2004) Signaling pathways in intestinal development and cancer, Annu Rev Cell Dev Biol 20, 695-723.
11. Hall, P. A., Coates, P. J., Ansari, B., and Hopwood, D. (1994) Regulation of cell number in the mammalian gastrointestinal tract: the importance of apoptosis, J Cell Sci 107 (Pt 12), 3569-3577.
12. Potten, C. S. (1998) Stem cells in gastrointestinal epithelium: numbers, characteristics and death, Philos Trans R Soc Lond B Biol Sci 353, 821-830.
13. Leedham, S. J., Brittan, M., McDonald, S. A., and Wright, N. A. (2005) Intestinal stem cells, J Cell Mol Med 9, 11-24.
14. Powell, D. W., Mifflin, R. C., Valentich, J. D., Crowe, S. E., Saada, J. I., and West, A. B. (1999) Myofibroblasts. II. Intestinal subepithelial myofibroblasts, Am J Physiol 277, C183-201.
15. Sansom, O. J., Reed, K. R., Hayes, A. J., Ireland, H., Brinkmann, H., Newton, I. P., Batlle, E., Simon-Assmann, P., Clevers, H., Nathke, I. S., Clarke, A. R., and Winton, D. J. (2004) Loss of Apc in vivo immediately perturbs Wnt signaling, differentiation, and migration, Genes Dev 18, 1385-1390.
16. Bienz, M., and Clevers, H. (2000) Linking colorectal cancer to Wnt signaling, Cell 103, 311-320.
17. Reya, T., and Clevers, H. (2005) Wnt signalling in stem cells and cancer, Nature 434, 843-850.

18. van Es, J. H., van Gijn, M. E., Riccio, O., van den Born, M., Vooijs, M., Begthel, H., Cozijnsen, M., Robine, S., Winton, D. J., Radtke, F., and Clevers, H. (2005) Notch/gamma-secretase inhibition turns proliferative cells in intestinal crypts and adenomas into goblet cells, Nature 435, 959-963.
19. Fre, S., Hannezo, E., Sale, S., Huyghe, M., Lafkas, D., Kissel, H., Louvi, A., Greve, J., Louvard, D., and Artavanis-Tsakonas, S. (2011) Notch lineages and activity in intestinal stem cells determined by a new set of knock-in mice, PLoS One 6, e25785.
20. Fre, S., Huyghe, M., Mourikis, P., Robine, S., Louvard, D., and Artavanis-Tsakonas, S. (2005) Notch signals control the fate of immature progenitor cells in the intestine, Nature 435, 964-968.
21. Rodilla, V., Villanueva, A., Obrador-Hevia, A., Robert-Moreno, A., Fernandez-Majada, V., Grilli, A., Lopez-Bigas, N., Bellora, N., Alba, M. M., Torres, F., Dunach, M., Sanjuan, X., Gonzalez, S., Gridley, T., Capella, G., Bigas, A., and Espinosa, L. (2009) Jagged1 is the pathological link between Wnt and Notch pathways in colorectal cancer, Proc Natl Acad Sci U S A 106, 6315-6320.
22. Imai, T., Tokunaga, A., Yoshida, T., Hashimoto, M., Mikoshiba, K., Weinmaster, G., Nakafuku, M., and Okano, H. (2001) The neural RNA-binding protein Musashi1 translationally regulates mammalian numb gene expression by interacting with its mRNA, Mol Cell Biol 21, 3888-3900.
23. Rezza, A., Skah, S., Roche, C., Nadjar, J., Samarut, J., and Plateroti, M. (2010) The overexpression of the putative gut stem cell marker Musashi-1 induces tumorigenesis through Wnt and Notch activation, J Cell Sci 123, 3256-3265.
24. McDonald, S. A., Preston, S. L., Lovell, M. J., Wright, N. A., and Jankowski, J. A. (2006) Mechanisms of disease: from stem cells to colorectal cancer, Nat Clin Pract Gastroenterol Hepatol 3, 267-274.
25. Li, L., and Clevers, H. (2010) Coexistence of quiescent and active adult stem cells in mammals, Science 327, 542-545.
26. Sangiorgi, E., and Capecchi, M. R. (2008) Bmi1 is expressed in vivo in intestinal stem cells, Nat Genet 40, 915-920.
27. Bjerknes, M., and Cheng, H. (1999) Clonal analysis of mouse intestinal epithelial progenitors, Gastroenterology 116, 7-14.
28. Barker, N., van Es, J. H., Kuipers, J., Kujala, P., van den Born, M., Cozijnsen, M., Haegebarth, A., Korving, J., Begthel, H., Peters, P. J., and Clevers, H. (2007) Identification of stem cells in small intestine and colon by marker gene Lgr5, Nature 449, 1003-1007.
29. Barker, N., Ridgway, R. A., van Es, J. H., van de Wetering, M., Begthel, H., van den Born, M., Danenberg, E., Clarke, A. R., Sansom, O. J., and Clevers, H. (2009) Crypt stem cells as the cells-of-origin of intestinal cancer, Nature 457, 608-611.
30. Harada, N., Tamai, Y., Ishikawa, T., Sauer, B., Takaku, K., Oshima, M., and Taketo, M. M. (1999) Intestinal polyposis in mice with a dominant stable mutation of the beta-catenin gene, EMBO J 18, 5931-5942.
31. Potten, C. S., Booth, C., Tudor, G. L., Booth, D., Brady, G., Hurley, P., Ashton, G., Clarke, R., Sakakibara, S., and Okano, H. (2003) Identification of a putative

intestinal stem cell and early lineage marker; musashi-1, Differentiation 71, 28-41.
32. Kayahara, T., Sawada, M., Takaishi, S., Fukui, H., Seno, H., Fukuzawa, H., Suzuki, K., Hiai, H., Kageyama, R., Okano, H., and Chiba, T. (2003) Candidate markers for stem and early progenitor cells, Musashi-1 and Hes1, are expressed in crypt base columnar cells of mouse small intestine, FEBS Lett 535, 131-135.
33. Sakakibara, S., Imai, T., Hamaguchi, K., Okabe, M., Aruga, J., Nakajima, K., Yasutomi, D., Nagata, T., Kurihara, Y., Uesugi, S., Miyata, T., Ogawa, M., Mikoshiba, K., and Okano, H. (1996) Mouse-Musashi-1, a neural RNA-binding protein highly enriched in the mammalian CNS stem cell, Dev Biol 176, 230-242.
34. Nakamura, M., Okano, H., Blendy, J. A., and Montell, C. (1994) Musashi, a neural RNA-binding protein required for Drosophila adult external sensory organ development, Neuron 13, 67-81.
35. Kawahara, H., Imai, T., Imataka, H., Tsujimoto, M., Matsumoto, K., and Okano, H. (2008) Neural RNA-binding protein Musashi1 inhibits translation initiation by competing with eIF4G for PABP, J Cell Biol 181, 639-653.
36. Battelli, C., Nikopoulos, G. N., Mitchell, J. G., and Verdi, J. M. (2006) The RNA-binding protein Musashi-1 regulates neural development through the translational repression of p21WAF-1, Mol Cell Neurosci 31, 85-96.
37. Sureban, S. M., May, R., George, R. J., Dieckgraefe, B. K., McLeod, H. L., Ramalingam, S., Bishnupuri, K. S., Natarajan, G., Anant, S., and Houchen, C. W. (2008) Knockdown of RNA binding protein musashi-1 leads to tumor regression in vivo, Gastroenterology 134, 1448-1458.
38. Li, D., Peng, X., Yan, D., Tang, H., Huang, F., Yang, Y., and Peng, Z. (2011) Msi-1 is a predictor of survival and a novel therapeutic target in colon cancer, Ann Surg Oncol 18, 2074-2083.
39. Lynch, H. T., and de la Chapelle, A. (2003) Hereditary colorectal cancer, N Engl J Med 348, 919-932.
40. Bodmer, W. F., Bailey, C. J., Bodmer, J., Bussey, H. J., Ellis, A., Gorman, P., Lucibello, F. C., Murday, V. A., Rider, S. H., Scambler, P., and et al. (1987) Localization of the gene for familial adenomatous polyposis on chromosome 5, Nature 328, 614-616.
41. Kinzler, K. W., Nilbert, M. C., Su, L. K., Vogelstein, B., Bryan, T. M., Levy, D. B., Smith, K. J., Preisinger, A. C., Hedge, P., McKechnie, D., and et al. (1991) Identification of FAP locus genes from chromosome 5q21, Science 253, 661-665.
42. Groden, J., Thliveris, A., Samowitz, W., Carlson, M., Gelbert, L., Albertsen, H., Joslyn, G., Stevens, J., Spirio, L., Robertson, M., and et al. (1991) Identification and characterization of the familial adenomatous polyposis coli gene, Cell 66, 589-600.
43. Ichii, S., Horii, A., Nakatsuru, S., Furuyama, J., Utsunomiya, J., and Nakamura, Y. (1992) Inactivation of both APC alleles in an early stage of colon adenomas in a patient with familial adenomatous polyposis (FAP), Hum Mol Genet 1, 387-390.

44. Levy, D. B., Smith, K. J., Beazer-Barclay, Y., Hamilton, S. R., Vogelstein, B., and Kinzler, K. W. (1994) Inactivation of both APC alleles in human and mouse tumors, Cancer Res 54, 5953-5958.
45. Kinzler, K. W., and Vogelstein, B. (1996) Lessons from hereditary colorectal cancer, Cell 87, 159-170.
46. Smith, K. J., Johnson, K. A., Bryan, T. M., Hill, D. E., Markowitz, S., Willson, J. K., Paraskeva, C., Petersen, G. M., Hamilton, S. R., Vogelstein, B., and et al. (1993) The APC gene product in normal and tumor cells, Proc Natl Acad Sci U S A 90, 2846-2850.
47. Horii, A., Nakatsuru, S., Ichii, S., Nagase, H., and Nakamura, Y. (1993) Multiple forms of the APC gene transcripts and their tissue-specific expression, Hum Mol Genet 2, 283-287.
48. Joslyn, G., Richardson, D. S., White, R., and Alber, T. (1993) Dimer formation by an N-terminal coiled coil in the APC protein, Proc Natl Acad Sci U S A 90, 11109-11113.
49. Seeling, J. M., Miller, J. R., Gil, R., Moon, R. T., White, R., and Virshup, D. M. (1999) Regulation of beta-catenin signaling by the B56 subunit of protein phosphatase 2A, Science 283, 2089-2091.
50. Kawasaki, Y., Senda, T., Ishidate, T., Koyama, R., Morishita, T., Iwayama, Y., Higuchi, O., and Akiyama, T. (2000) Asef, a link between the tumor suppressor APC and G-protein signaling, Science 289, 1194-1197.
51. Munemitsu, S., Albert, I., Souza, B., Rubinfeld, B., and Polakis, P. (1995) Regulation of intracellular beta-catenin levels by the adenomatous polyposis coli (APC) tumor-suppressor protein, Proc Natl Acad Sci U S A 92, 3046-3050.
52. Rubinfeld, B., Souza, B., Albert, I., Muller, O., Chamberlain, S. H., Masiarz, F. R., Munemitsu, S., and Polakis, P. (1993) Association of the APC gene product with beta-catenin, Science 262, 1731-1734.
53. Su, L. K., Vogelstein, B., and Kinzler, K. W. (1993) Association of the APC tumor suppressor protein with catenins, Science 262, 1734-1737.
54. Kishida, S., Yamamoto, H., Ikeda, S., Kishida, M., Sakamoto, I., Koyama, S., and Kikuchi, A. (1998) Axin, a negative regulator of the wnt signaling pathway, directly interacts with adenomatous polyposis coli and regulates the stabilization of beta-catenin, J Biol Chem 273, 10823-10826.
55. Beroud, C., and Soussi, T. (1996) APC gene: database of germline and somatic mutations in human tumors and cell lines, Nucleic Acids Res 24, 121-124.
56. Neufeld, K. L. (2009) Nuclear APC, Adv Exp Med Biol 656, 13-29.
57. Zhang, F., White, R. L., and Neufeld, K. L. (2000) Phosphorylation near nuclear localization signal regulates nuclear import of adenomatous polyposis coli protein, Proc Natl Acad Sci U S A 97, 12577-12582.
58. Henderson, B. R. (2000) Nuclear-cytoplasmic shuttling of APC regulates beta-catenin subcellular localization and turnover, Nat Cell Biol 2, 653-660.
59. Rosin-Arbesfeld, R., Townsley, F., and Bienz, M. (2000) The APC tumour suppressor has a nuclear export function, Nature 406, 1009-1012.
60. Anderson, C. B., Neufeld, K. L., and White, R. L. (2002) Subcellular distribution of Wnt pathway proteins in normal and neoplastic colon, Proc Natl Acad Sci U S A 99, 8683-8688.

61. Narayan, S., Jaiswal, A. S., and Balusu, R. (2005) Tumor suppressor APC blocks DNA polymerase beta-dependent strand displacement synthesis during long patch but not short patch base excision repair and increases sensitivity to methylmethane sulfonate, J Biol Chem 280, 6942-6949.
62. Wang, Y., Azuma, Y., Moore, D., Osheroff, N., and Neufeld, K. L. (2008) Interaction between tumor suppressor adenomatous polyposis coli and topoisomerase IIalpha: implication for the G2/M transition, Mol Biol Cell 19, 4076-4085.
63. Wang, Y., Coffey, R. J., Osheroff, N., and Neufeld, K. L. (2010) Topoisomerase IIalpha binding domains of adenomatous polyposis coli influence cell cycle progression and aneuploidy, PLoS One 5, e9994.
64. Spears, E., and Neufeld, K. L. (2011) Novel double-negative feedback loop between adenomatous polyposis coli and Musashi1 in colon epithelia, J Biol Chem 286, 4946-4950.
65. http://www.stanford.edu/group/nusselab/cgi-bin/wnt/target_genes
66. http://www.cancer.org/Cancer/ColonandRectumCancer

Chapter 2

Contribution of the Apc/Msi1 Double-Negative Feedback Loop to Intestinal Cell Homeostasis in Mice

Abstract

Colorectal cancer is proposed to arise due to misregulation of stem cells in the intestinal epithelium. Adenomatous Polyposis Coli (APC) truncating mutations have been implicated as the initiating event in 80% of colorectal cancers. Musashi1 (MSI1), a translational inhibitor, has been found to be important in stem cell regulation. Previously, the Neufeld lab identified a double-negative feedback loop between APC and MSI1, i*n vitro*, using human colon cell lines. APC regulates MSI1 via Wnt signaling and MSI1 targets APC mRNA for translational inhibition. Though both APC and MSI1 have been found to be important in tumorigenesis, the implication of this double-negative feedback loop on stem cell regulation and tumorigenesis is unknown. We hypothesize that this double-negative feedback loop is key to maintaining balance between proliferation and differentiation *in vivo*. To address the role of the APC/MSI1 double-negative feedback loop *in vivo*, we are characterizing Msi1 knockout mice for phenotypes associated with disruption of this feedback loop in both the small intestine and colon. When comparing the small intestine of Msi1 knockout mice to wild-type mice, we found down-regulation of Wnt target gene transcripts and lower Apc protein levels. Proliferation remained unchanged as did goblet cell differentiation. An *ex vivo* culture system produced less crypt-like protrusions from $Msi1^{-/-}$ organoids. Apoptosis appeared to be reduced in $Msi1^{-/-}$ small intestinal epithelia. When comparing the colons of Msi1 knockout mice and wild-type mice, Wnt target gene expression was unaltered as were Apc protein levels. However, proliferation was reduced in $Msi1^{-/-}$ colons as was crypt

fission. Apoptosis was unaffected. We propose that disregulation of the APC/MSI1 double-negative feedback loop leads to disruption of homeostasis in the small intestine whereas in the colon it may not play an integral role.

Introduction

The intestinal system is one of the most rapidly renewing tissues in the body and thus needs many levels of regulation in order to maintain homeostasis. The intestine is composed of two stem cell populations that reside near the base of the crypt and that undergo asymmetric division to give rise to all differentiated cells of the intestine. "Active" (Lgr5-positive) stem cells are located at the crypt base, whereas "quiescent" (Bmi1-positive) stem cells reside in the +4 position above the crypt bottom (Figure 1.1). The daughter cells produced through asymmetric division travel upward from the crypt base and upon reaching the crypt-villus junction further differentiate into the secretory or absorptive cells. Paneth cells are the only differentiated cell type to move to the crypt bottom, where they help to maintain the stem cell niche (*1*). Misregulation of intestinal homeostasis via mutation of either stem cell population has been shown to initiate adenoma formation, which may eventually progress to colorectal cancer (*2, 3*).

Mutation of *APC* is the initiating event in ~80% of all sporadic colorectal cancers and germ-line *APC* mutations are associate with the syndrome familial adenomatous Polyposis (FAP). Persons with FAP have hundreds to thousands of colonic polyps by early adolescence and colon cancer by middle age if their colon is

not removed. A role for APC in tumorigenesis is linked to its function as a negative regulator of the canonical Wnt pathway where APC acts as a scaffold protein in a destruction complex that targets transcription factor β-catenin for proteasomal degradation. Wnt signaling is important to maintain the stem cell niche in the intestine; secreted Wnt signal allows progenitors to maintain a proliferative stem-like state. Conditional loss of Apc in adult mice leads to increased size of the progenitor compartment, more proliferative cells and more undifferentiated cells. These mice also had increased expression of the RNA-binding protein Musashi1 (Msi1) (*4*).

Msi1 has previously been shown to be a stem cell marker in the intestine (*5*) and has also been linked to maintaining cells in a progenitor state. Msi1 is known for its role as a translational inhibitor of *m-numb*, an inhibitor of the Notch pathway, which allows for activation of Notch and maintenance of cells in a non-differentiated state (*6*). Msi1 has also been shown to be an inhibitor of $p21^{WAF-1}$ allowing neural cells to be maintained in an actively cycling state (*7*). Ultimately, both Msi1 and APC participate in the balance of proliferation versus differentiation in the intestine.

Previous work in our lab showed a negative feedback loop between APC and Msi1 in cultured cells. APC is an inhibitor of MSI1 (*8*) and this inhibition involved the Wnt pathway (*9*). MSI1, in turn, inhibits translation of APC (*8*). To date, the studies supporting a double-negative feedback loop between APC and MSI1 were performed in cultured cells. Therefore, it is unknown how this double-negative feedback loop affects the homeostasis of intestinal tissue or whether disruption of this feedback loop disrupts the balance between proliferation and differentiation in

the intestine. To investigate this feedback loop *in vivo*, we utilized Msi1$^{-/-}$ mice to examine phenotypes related to disruption of this feedback loop and the effects on Wnt signaling in both the small intestine and the colon. These mice were generated in the Okano lab by using a targeting construct to delete the entire Msi gene. Msi knockout in these mice lead to abnormal brain development but are not lethal (*10*). However, phenotypes in the intestine caused by Msi knockout have not been examined. We hypothesized that in this model, Msi1 deletion would lead to increased levels of Apc, causing a subsequent decrease in Wnt signaling. In the current study, we demonstrate that the small intestine and colon display distinct phenotypes in mice with Msi1 deletions. In the small intestine, Apc protein levels in Msi1$^{-/-}$ mice were slightly elevated Wnt target genes were downregulated. Proliferation was unaffected, though crypt fission was decreased. Goblet cell differentiation was unaffected and apoptosis was decreased. In the colon, no change was seen in Apc protein expression or Wnt target gene expression. Proliferation was found to decrease though crypt fission was found to increase. Apoptosis was unaffected. These results suggest that the Msi1/Apc negative feedback loop in the small intestine of mice plays a role in intestinal homeostasis while Msi1 loss in the colon leads to phenotypes not related to Wnt signaling.

Materials and Methods

Mouse Husbandry

ICR129 Msi1$^{-/-}$ mice in CD-1 background were a kind gift from the Okano lab and were used for this study. Briefly, Msi1$^{-/-}$ mice were generated by replacing 4 exons of the *msi1* gene, including the initiation codon, with a Neo cassette through homologous recombination. Msi1 knockout was confirmed by Western blot (*10*). Apc^{1322T} mice from Ian Tomlinson in C57BL6 background.

Mouse Genotyping

After weaning, mice were identified with a metal ear tag. In order to determine genotype, tail DNA was isolated from the mice and the PCR protocol from Riken BRC PCR protocol RBRC04435 was used. Primer sets used to genotype mice for *Msi1* knockout allele (5'-CTGAGCTATCTCCAACCCGACCCAG-3' and 5'-TCCAGACTGCCTTGGGAAAAAGCGCCT-3'; 280 bp) and wild-type allele (5'-TGAAAGAGTGTCTGGTGATGCGGGAC-3' and 5'-TTGGAGTCGAGCTCGTGCCGCGATT-3'). Two separate reactions were run simultaneously for each mouse including the *Msi1* knockout primers and wild-type primers. Reaction conditions were as follows: 94°C for 3 minutes, 94°C for 30 seconds, 60°C for 30 seconds, 72°C for 1 minute, and 72°C for 5 minutes.

Isolation of mouse intestinal epithelial cells

Small Intestine, from below the stomach to the cecum, and colon, including cecum, was removed from 10-11 week old mice. In order to isolate intestinal epithelia cells, small intestine and colon were opened longitudinally. Each intestinal piece was placed into a 50 mL conical tube containing cell isolation buffer (3 mM EDTA, 0.5mM

dithiothreitol (DTT)) and incubated for 90 minutes room at temperature. Intestinal pieces were removed from cell isolation buffer, and placed into 15 mL conicals containing 12 mL of PBS and shaken vigorously for 20 seconds to release epithelial cells. Intestinal pieces were removed from tubes prior to centrifugation at 700 g for 5 min to pellet cells. Crypt supernatants were removed and pellets were resuspended in 5 mL PBS for the small intestine and 2.5 mL PBS for the colon. One ml and 300 μL aliquots of each cell suspension were placed into fresh microfuge tubes and centrifuged at 15,800 g and supernatant was removed. The pellet from the 1 mL aliquot was resuspended in 1 mL of Trizol (Invitrogen) and stored at -80°C to be used for RNA analysis. The pellet from the 300 μL aliquot was resuspended in 5x sample buffer (25% glycerol, 3.12 mM Tris-HCL pH=6.8, 10% w/v sodium dodecyl sulfate, 0.0027% bromphenol blue in ethanol for color, 5% 2-mercaptoethanol) and heated at 100°C for 2 min, vortexed, heated again at 100°C for 2 min and stored at -80°C to be used for immunoblot analysis.

Immunohistochemistry of intestinal epithelia

Jejunums from the small intestine and the whole colon excluding the cecum were isolated from 13 week old mice of each genotype. Tissue was fixed in 10% saline-buffered formalin overnight (less than 24 hours) at 4°C and then stored in 70% ethanol for 24 hours at 4°C. Tissues were embedded in paraffin and sectioned at 8 μm. Immunohistochemistry for Ki-67 was performed using the histomouse kit (Invitrogen cat. No. 95-9541) according to the manufacturer's protocol and were

incubated with rat anti-mouse Ki-67 antibody (1:20 Dako cat. No. M7249) overnight. Sections were counterstained with hematoxylin and coded for blind scoring. 48-50 crypts 75-145 μm in length in the jejunum tissue samples and 27-100 crypts 75-145 μm in length in the colon samples were scored for Ki-67-postive cells using the 20x objective and a Zeiss Axiovert 135 microscope. The average of all samples/crypt were evaluated for significance using unpaired, two-tailed t-tests calculated by Microsoft Excel. Representative images of crypts were captured using the 40x objective on Nikon Eclipse 80i microscope with Optronics Magnafire SP digital camera and acquired with Magnafire software.

Scoring goblet cells.

Jejunum was isolated from 4 mice of each genotype at 12 weeks of age. Processing of tissue was performed as in *immunohistochemistry of intestinal epithelia*. A protocol adapted from IHCworld.com for alcian blue staining was followed. Tissue was deparafinized and rehydrated in an ethanol series followed by staining with alcian blue for 30 minutes to stain goblet cells. Tissue was then dehydrated through an ethanol series and xylene washing and mounted with xylene mounting medium and coded for blind scoring. Images of representative jejunum were captured with the 10x objective on Nikon Eclipse 80i microscope with Optronics Magnafire SP digital camera and acquired with Magnafire software. The bottom 183 μm of each villi was scored for 26-58 villi per $Msi1^{+/+}$ and 21-68 villi per $Msi1^{-/-}$ mouse. The average

number of alcian blue-positive cells was calculated for each mouse and evaluated for significance using unpaired, two-tailed t-tests calculated by Microsoft Excel.

Immunoblot analysis

Protein samples were separated by polyacrylamide gel electrophoresis and transferred to a nitrocellulose membrane. Blots were blocked with 5% non-fat dry milk/TBST and probed in this solution as well. Blots were probed with the following primary antibodies: rabbit anti-APC M2 1:3000 (*11*), mouse anti β-actin 1:3000 (Sigma), and rabbit anti-histone H2A.x 1:3000(Abcam #ab11175). Secondary antibodies used included: horseradish peroxidase goat anti-rabbit IgG (Bio-Rad cat. No. 172-1019) and HRP-rabbit anti-mouse IgGγ (Zymed cat. no. 61-6020). Blots were developed using SuperSignal West Femto Maximum Sensitivity Substrate (Pierce) and a Kodak Image Station 4000R. Band intensity was analyzed using Kodak ID Image Analysis Software and sum integer values were used. Apc protein band intensity was first normalized to β-actin and values for $Msi1^{+/+}$ were set to 1. When evaluating apoptosis, β-fractin band intensity was normalized to histone H2A.x. Values for $Msi1^{+/+}$ were set to 1 in all experiments. The p-values were calculated by two-tailed Mann-Whitney non-parametric test.

Crypt fission analysis

For small intestine: the distal 1 cm of tissue was removed, opened longitudinally and incubated in 30mM EDTA in PBS solution on ice for 20 min. The intestine was washed once in PBS, added to 25 mL of PBS, and shaken for 5 min at 3 shakes/second to dissociate crypts and villi. The intestinal piece was removed and the solution was filtered through a 70 μm filter to remove villi. An aliquot of 100 μL was removed and scored using light microscopy with the 16x objective on a Zeiss Axiovert 135 microscope. Representative images were taken on the same microscope with the Hamamatsu digital camera 610600 ORCA-R^2 and acquired with HCImage Live V3.0 software. Crypts undergoing fission were scored as a percent of the total crypts counted/mouse and the data from each mouse of a given genotype were averaged. The p-values were calculated by two-tailed Mann-Whitney non-parametric test.

For colon: the distal 1 cm of colon was removed, opened longitudinally, and incubated in 30 mM EDTA solution in PBS on ice for 20 min. The colon piece was removed from EDTA solution, placed into 500 μL of PBS, and shaken vigorously for 5 minutes. A 100 μL aliquot was removed scored as for the small intestine using the same microscope and camera for pictures and data collection.

Crypt Organoid Culture system

One mouse of each genotype was culled at 5 weeks of age and the small intestine removed. The small intestine was opened longitudinally, washed 3x with cold HBSS

(Calcium and magnesium free) and cut into ~ 1 cm pieces. The pieces were placed into 30 mM EDTA/PBS and allowed to incubate on ice for 20 min. EDTA solution was removed and tissue was washed with 50 mL of cold HBSS. After the HBSS wash,25 mL of cold HBSS was added to the tissue. Intestinal pieces were shaken for 5 min at 3 shakes/second to dissociate crypts and villi. Solution containing crypts and villi was poured through a 70 μm filter to remove villi. The solution was then centrifuged at 250 g for 5 min to pellet crypts and supernatant was removed. Crypt pellets were resuspended in 25 mL of basal media including: advanced DMEM-F12 (Gibco cat. no. 12634-010), 200 mM L-glutamine, 10 mM Hepes pH 7.5. Crypt solutions were centrifuged at 200 g and most of supernatant was removed leaving 2 mL in which crypt pellet was resuspended. Using wide-bore pipettes 40 μL of crypt solution was added to 40 μL of basal media in 5% BSA coated-microfuge tubes (crypts diluted 1:2). 80 μL of matrigel (BD matrigel basement membrane matrix growth factor reduced, cat. no. 354230) was added to crypt solution (crypts:matrigel = 1:1). 40 μL of crypt-matrigel solution was plated directly to the center of the well (without allowing solution to touch sides of the well) in 24 well plates and incubated for 20 min at 37°C with 5% carbon dioxide to allow matrigel to solidify. Once solidified, 400 μL of overlay was added to each well and incubated at 37°C with 5% carbon dioxide for the duration of the experiment. Overlay included: 100 ng/mL Noggin (Peprotech cat. no. 250-38), 10 ng/mL of EGF (Peprotech cat. no. PMG8044), 500 ng/mL R-spondin1 (Sino Biological cat. no. 50316-M08H), 1 x Penicillin-Streptomycin (Gibco cat. no. 15140-148) in basal media. Organoids formed from plated crypts and protrusions were scored beginning one day (24

hours) after plating using a dissecting scope to count the number of protrusions on each organoid. For $Msi1^{-/-}$ and $Msi1^{+/+}$ cultures, all organoids were scored in all wells for protrusions, 10-662 organoids in $Msi1^{-/-}$ cultures and 78-495 in $Msi1^{+/+}$ cultures. In $Apc^{1322T/+}$ cultures, 5 non-overlapping views were scored in each well for organoids. In the $Apc^{1322T/+}$ culture, 207-802 organoids were scored for protrusions and in the $Apc^{+/+}$311-1061 organoids were scored. The data for the Msi1 culture is presented as a box-and-whisker plot, while the data for the $Apc^{1322T/+}$ culture is presented as the average protrusions/organoid. The cultures were prepared from one mouse per genotype total. Significance was calculated using a student t-test.

In the Msi1 crypt culture, organoids were passed on day 9 after initial plating. Passaging was performed by removing crypts and media from 3 wells by pipetting vigorously and scraping matrigel with pipette tip to dislodge from the well bottom and combining crypt solutions into 5% BSA-coated microfuge tubes. Crypt solutions were centrifuged at 200 g and pellets containing organoids were resuspended in 100 μL of matrigel and 40 μL of suspension was added to each well of a 24 well plate. Plates were then kept at 37°C with 5% carbon dioxide to allow matrigel to solidify for 20 min. 400 μL of overlay was added to crypts and crypts were scored each day for protrusions until organoid number fell below 10 organoids in the $Msi1^{-/-}$ cultures.

Analysis of mRNA by real-time reverse transcription-PCR

RNA was prepared from intestinal epithelial cells isolated from $Msi1^{+/+}$ and $Msi1^{-/-}$ mice as described in the section *Isolation of mouse intestinal epithelial cells* and rt-PCR was performed to analyze Wnt target genes as described in (*12*).

Results in the small intestine

APC protein levels increased in $Msi1^{-/-}$ mice.

To investigate whether the APC/MSI1 double-negative feedback loop was maintained in the small intestine, we used $Msi1^{-/-}$ mice generated in the Okano lab, which have a germ-line deletion of Msi1(*10*). We hypothesized that in this model, Apc levels would increase due to an alleviation of translational repression mediated by Msi1. To test this hypothesis, we isolated protein from small intestinal epithelial cells and examined Apc protein levels via immunoblot. Apc protein levels in $Msi1^{-/-}$ mice increased with respect to $Msi1^{+/+}$ mice, though not significantly (Fig. 2.1A and 2.1B). This result suggests that the absence of Msi1 does significantly affect Apc protein levels when combining the entire small intestinal epithelia. However, the slight increase in this total Apc level leaves open the possibility that the Apc/Msi1 double-negative feedback loop is maintained in only a subset of small intestinal cells.

Wnt target gene expression is down-regulated in $Msi1^{-/-}$ mice.

Because a slight elevation in Apc level was seen in the small intestine of Msi1$^{-/-}$ mice, we examined the effect of disrupting Apc/Msi1 double-negative feedback regulation on Wnt target genes. Apc is a negative regulator of Wnt signaling and therefore, was expected to have an inhibitory effect on the expression of Wnt target genes. To evaluate Wnt target gene expression, we isolated mRNA from intestinal epithelial cells and quantified the relative expression of four canonical Wnt target genes (Figure 2.2). Three genes upregulated by the canonical Wnt pathway, *c-Myc* , *axin-2*, and *cyclin-D1*, showed lower expression in Msi1$^{-/-}$ mice than in Msi1$^{+/+}$ mice. *BTEB2*, a gene regulated by non-canonical Wnt signaling, showed no change in expression. Unexpectedly, *Hath-1*, a gene down-regulated by canonical Wnt signaling showed no significant alteration in expression levels between Msi1$^{-/-}$ and Msi1$^{+/+}$ mice.

No significant change in proliferation in intestinal epithelia of Msi1$^{-/-}$ mice.

Due to decreased Wnt signaling, we expected to see a subsequent decrease in proliferation in the small intestine. In order to examine proliferation, immunohistochemistry was performed on paraffin-embedded jejunum from mice using Ki67 as a proliferation marker. Unexpectedly, crypts showed no significant change in proliferating cells/crypt between Msi1$^{-/-}$ and Msi1$^{+/+}$ mice (Figure 2.3).

No significant change in Goblet cell differentiation in small intestine of Msi1$^{-/-}$ mice.

Inhibition of the Wnt signaling pathway has been shown to ablate differentiation of secretory cells in the small intestine such as goblet cells (*13*). Because Wnt target genes were inhibited in $Msi1^{-/-}$ mice, we next examined the effect of Msi1 knockout on goblet cell differentiation in the small intestine. Jejunum was isolated from the mice, paraffin embedded, and stained with alcian blue, a marker for goblet cells. Unexpectedly, no significant change was detected in the number of goblet cells in villi between $Msi1^{-/-}$ and $Msi1^{+/+}$ mice.

Elevation of crypt fission in the small intestine of $Msi1^{-/-}$ mice.

Crypt fission is a mechanism by which crypts are proposed to spread throughout the intestine in a short postnatal period. In mice, crypt doubling peaks within the first three months of life. Crypts will then undergo fission only gradually with age. Crypt fission is a proposed to result from an expansion of stem cell populations that causes an increase in proliferating cells, resulting in a structurally unstable crypt. When a threshold number of stem cells are exceeded in the crypt, the crypt will undergo fission (*14*). A crypt undergoing fission will bifurcate at the bottom and eventually produce two daughter crypts (Figure 2.5A). Thus crypt fission can be used as an epiphenomenon of stem cell number (*14*).

In $Msi^{-/-}$ mice, we predicted a decrease in crypt fission because Msi1 has been shown play an active role in maintaining stem cell division in neural cells (*15*). In order to examine effects of Msi1 knockout on stem cell populations in the intestine, we looked at crypt fission in both mice populations by scoring isolated crypts for

crypt fission (Figure 2.5B). Unexpectedly, crypts in Msi1$^{-/-}$ mice had significant elevation in crypt fission compared to Msi1$^{+/+}$ mice (Figure 2.5C).

Decrease in protrusions/organoid in Msi1$^{-/-}$ mice.

As a second method to determine crypt cell population differences in mice of both genotypes, we used an *ex vivo* culture system of isolated small intestinal crypts from the mice. In this system adapted from Sato et al., 2009 and David Sackville's thesis, crypts are removed from surrounding mesenchymal tissue, separated from villi, and plated in a laming-rich 3D media, matrigel. The crypts are provided with external signals. R-spondin1, a critical component of this external signals mixture, enhances Wnt signaling allowing crypts to continue to proliferate (*16*). Once the crypts are in culture, they produce organoid structures, with differentiated secretory and absorptive cells present along the luminal surface of the organoid. After 24 hours in culture, the organoids will produce new crypt-like protrusions from stem cells (refer to schematic, Figure 2.6A) (*17*). Because protrusions arise from stem cells, counting the number of protrusions per organoid would be a way to determine general differences in stem cell populations.

To provide proof of concept that this *ex vivo* culture system could be used to determine stem cell population differences, we first cultured crypts isolated from an APC$^{1322T/+}$ mouse and a wild-type mouse. A previous study using the APC$^{1322T/+}$ mouse model showed that these mice have a higher Lgr5+ stem cell population than wild-type mice (*18*). After culturing APC$^{1322T/+}$ organoids for five days, APC$^{1322T/+}$ had significantly more protrusions than wild-type organoids (2.6B).

Because Msi1 overexpression has been correlated to expansion of stem cell populations (*9*), we expected that knockout of Msi1, in this culture system, would produce organoids with fewer protrusions. In order to ascertain stem cell population differences, we allowed crypts to grow in culture and counted protrusions on each organoid. After 8 days of growth, crypts from $Msi1^{-/-}$ mice had less protrusions per organoid than $Msi1^{+/+}$ mice (Figure 2.7A). By day nine, organoids were obscured from vision by dead debris in culture, so organoids were passaged to allow for new protrusions to grow and be scored. Scoring commenced immediately following passage and again $Msi1^{-/-}$ mice had less protrusions per organoid than $Msi1^{+/+}$ mice (Figure 2.7B).

Apoptosis in the small intestine of $Msi1^{-/-}$ mice.

Previous reports describe an increase in apoptosis upon conditional knockout of APC in adult mice (*4, 19*). Therefore, we hypothesized that elevated levels of Apc would decrease apoptosis in $Msi1^{-/-}$ mice. In order to examine apoptosis in these mice, western blot analysis of β-fractin, a cleavage product of β-actin during apoptosis, were quantified in both genotypes. β-fractin levels were found to be decreased in $Msi1^{-/-}$ mice, though this trend did not reach significance (Figure 2.8A and 2.8B).

Discussion

Previous work in the lab demonstrated a double-negative feedback loop between APC and MSI1 in cell culture (*8*). However, the effects of this feedback loop have not been demonstrated in intestinal tissue. In this study, we utilized a mouse model generated in the Okano lab with ablated endogenous Msi1 (*10*) in order to study phenotypes related to Wnt signaling due to loss of Msi1 in the intestine. Here we present data for the small intestine that shows that Apc protein levels are up and three Wnt target genes (*cyclin-D1, c-myc, and axin-2*) are downregulated in the small intestine. The absence of Msi1 would be expected to alleviate translational repression of Apc and Apc's role as a downregulator of the canonical Wnt pathway would explain the subsequent downregualtion of Wnt target genes. This data implicates the Apc-Msi1 feedback loop in homeostasis of the small intestine.

Surprisingly, Hath1, a gene shown to be downregulated by canonical Wnt signaling, did not show a response to increased levels of Apc protein.
Hath1 was shown to be downregulated by the Wnt pathway (*20*) and was also shown to be upregulated when a repressor of Notch, Numb, was knocked-down in colon cancer cell lines (*21*). Therefore, it would have been expected that elimination of Msi1, which translationally represses Apc, thus downregulating the Wnt pathway and Numb, which inhibits the Notch pathway, would result in an increase in Hath1 transcript. However, this was not seen. This result could be due to competition between signaling pathways in the intestine. For instance, one study found that in neural precursor cells, Hath1 was upregulated by β-catenin upon inhibition of Notch signaling (*22*). In our system, Msi1 knockout led to APC increase. Inhibition of β-catenin would be expected and thereby a decrease in Hath1 transcription. However,

it would also be predicted that Msi1 knockout, leading to inhibition of Notch, would upregulate Hath1. Therefore, these two regulatory mechanisms may compensate for one another, leading to no change in Hath1 overall. Further investigation into the regulatory mechanisms underlying Hath1 expression still need to be investigated.

Other unexpected results included that proliferation of intestinal cells and differentiation of goblet cells was unchanged in Msi1$^{-/-}$ mice. Proliferation is a downstream effect of Wnt signaling and is usually restricted to the progenitor compartment of the intestine. In Msi1$^{-/-}$ mice, it appeared that proliferating cells were still maintained in the progenitor compartment and overall proliferation as scored by Ki-67 staining was unchanged. In the future a secondary method of assessing proliferation would need to be utilized such as injecting mice with BrdU, which would allow for detection of cells entering S-phase over a period of time. A secondary method would yield more confidence in these results.

Goblet cell differentiation also showed no change in Msi1$^{-/-}$ mice. Goblet cells have been shown to be lost upon conditional knockout of Apc in the small intestine (*4*). Therefore, goblet cells would have been expected to increase due to increased Apc protein levels in Msi1$^{-/-}$ mice. However, the number of alcian blue positive cells was not found to change in these mice. Hath1 has also been shown to be associated with a goblet cell phenotype in the small intestine(*23*). In our previous experiment of Wnt target gene levels, Hath1 transcript levels were shown not to be affected by loss of Msi1. Therefore, the connection between Hath1 and goblet cells may not be affected by loss of Msi1.

Though proliferation and differentiation of goblet cells appeared to be unaffected, loss of Msi1 appeared to have a contradictory effect on crypt fission and the number of protrusions/organoid in an *ex vivo* crypt culture. Crypt fission, an indirect measurement, would be expected to decrease with loss of Msi1 because of Msi1's role in stem cell division. However, it was observed during the crypt isolation procedure that shaking the crypts from the small intestine may not have produced whole crypts, but rather pieces of crypts. For the small intestine, it was noticeably harder to dissociate crypts from surrounding tissue and more vigorous dissociation methods had to be employed than in the colon. The method of isolating crypts from the small intestine may have damaged crypts emerging and thereby made scoring inaccurate. An alternative method to score crypt fission in the small intestine should be sought.

Given the difficulties encountered when isolating whole crypts for crypt fission analysis, a second method, an ex vivo culture system, was employed to evaluate stem cell population differences between the two genotypes. This method allows for crypts isolated from the small intestine to form organoids in culture. These organoids will then grow crypt-like protrusions from stem cells (*17*) and protrusion number was scored as a way to capture differences between the populations. The median number of protrusions from $Msi^{-/-}$ organoids was consistently lower than from $Msi^{+/+}$ organoids over an eight day period. After passaging, the median of the $Msi^{-/-}$ culture was relatively similar to that of the $Msi^{+/+}$ culture, however, the number of organoids scored in the culture was very small (10 organoids on day 15) and may not have been representative.

Finally, decreased apoptosis in the $Msi^{-/-}$ mice was an unexpected finding. Msi1 knock-down in HCT116 cells showed an increase in apoptosis (*24*). However, in these experiments, the HCT116 cell line has a stabilizing mutation in β-catenin and therefore the Wnt pathway is constitutively activated. Therefore Msi1's role in apoptosis may have been through other pathways not related to Wnt signaling.

In summary, the Msi1/Apc double-negative feedback loop appears to affect the small intestine, though this effect does not fit with previously seen phenotypes involving disruption of Wnt signaling. This study provides a starting point to determine phenotypes associated with loss of this regulatory mechanism and in the future could be used to understand the role of Msi1 in an Apc-mutant background.

In the next section, we will summarize the effects of loss of Msi1 seen in the colon as they are different than those found in the small intestine. A summary of results found in both large and small intestine can be found in Table 2.1.

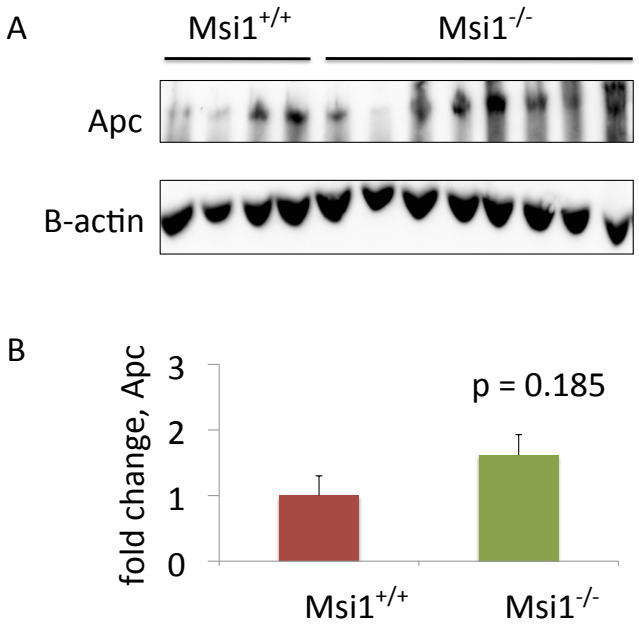

Figure 2.1. ***Apc protein levels in the small intestine.*** **(A) Representative blots of Apc protein levels in Msi1$^{-/-}$ mice. Apc levels were found to be higher in the small intestine of Msi1$^{-/-}$ mice, although it did not reach statistical significance (p= 0.185). (B) Protein was isolated from epithelial cells of the small intestines of 4 Msi1$^{+/+}$ and 10 Msi1$^{-/-}$ mice. APC band intensities were normalized to β-actin and are presented as average fold change relative to Msi1$^{+/+}$ mice +/- s.e.m. P-values < 0.05 as calculated by the Mann-Whitney non-parametric test are considered significant.**

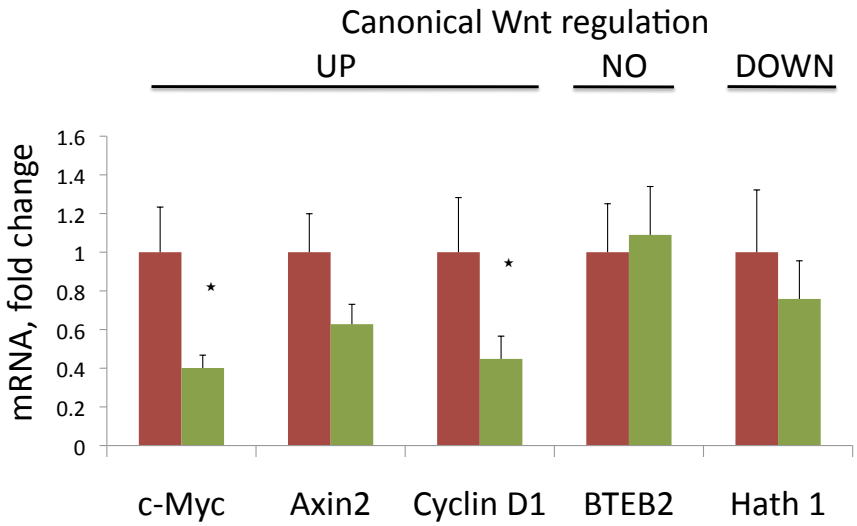

Figure 2.2. ***Down regulation of Wnt target genes in the small intestine of Msi1$^{-/-}$ mice.*** **Small Intestinal epithelial cells were isolated from the small intestine of Msi1$^{+/+}$ mice and Msi1$^{-/-}$ mice. For each sample, mRNA levels were examined for three genes upregulated by Wnt signaling, *c-Myc*, *Axin2*, and *CyclinD1*, by reverse transcriptase-PCR. As controls, mRNA from one gene not regulated by Wnt signaling,*BTEB2*, and one gene downregulated by Wnt signaling, *Hath1*, were examined. Each gene was normalized to HGPRT, a housekeeping gene. The results from 5-10 mice are presented as the average mRNA fold change relative to Msi1$^{+/+}$ mice +/- s.e.m. P-values < 0.05 as calculated by the Mann-Whitney non-parametric test are considered significant and are indicated by an asterisk.**

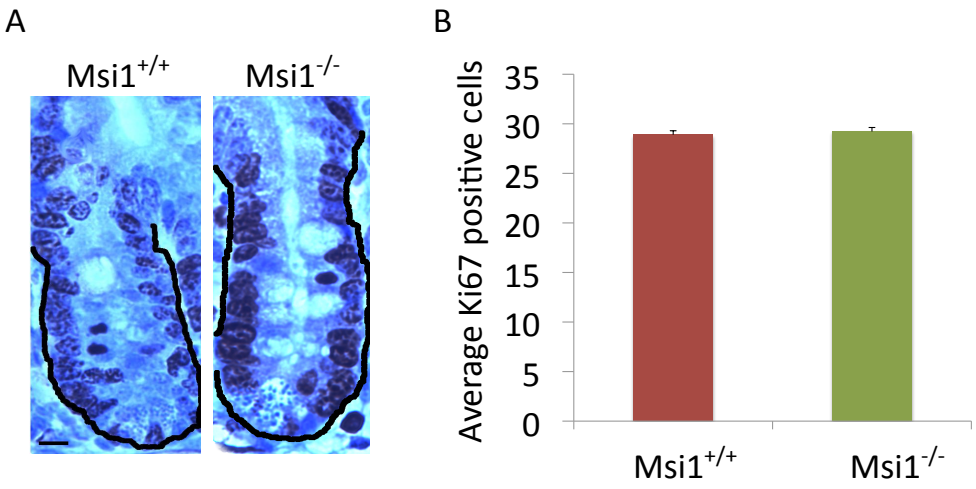

Figure 2.3. ***Proliferation in the jejunum of Msi1$^{-/-}$ mice is unchanged compared to Msi1$^{+/+}$ mice.*** **(A) Representative images of cypts from Msi1$^{+/+}$ (left) and Msi1$^{-/-}$ (right) with the black line indicating crypt border. Scale bar = 10 um (left panel). Jejunums were collected from 4 mice of each genotype and paraffin embedded. 48-50 crypts 75um-145um in length were scored per mouse. (B) Data is presented as the average number of cells positive for proliferation marker Ki67 per crypt +/- s.e.m for all samples. Proliferation differences between Msi1$^{-/-}$ compared to Msi1$^{+/+}$ were found to not be significant (p-value: 0.564) as calculated by the student t-test.**

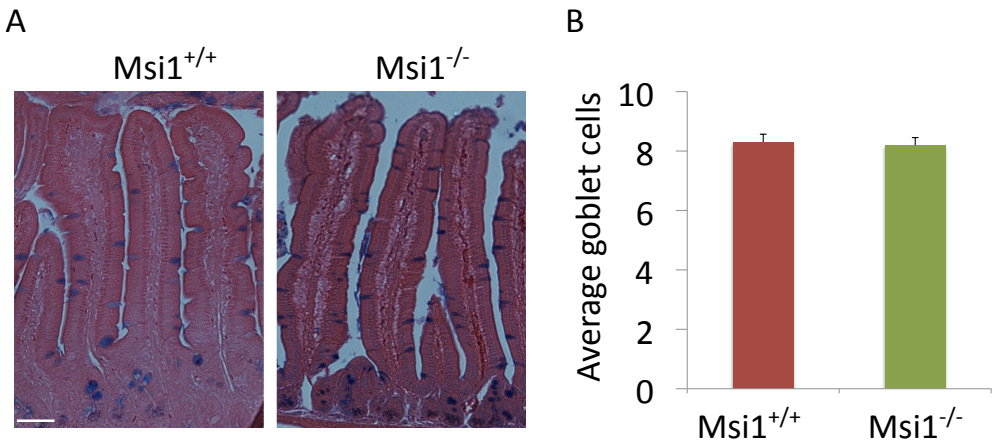

Figure 2.4. ***Goblet cell differentiation in the jejunum of Msi1$^{-/-}$ mice is unchanged compared to Msi1$^{+/+}$ mice.*** **Immunohistochemical analysis was performed on the jejunums of 4 Msi1$^{+/+}$ mice and 4 Msi1$^{-/-}$ mice using Alcian blue staining as a marker for goblet cells. (A) Representative images of isolated intestinal tissue from Msi1$^{+/+}$ and Msi1$^{-/-}$ mice stained with Alcian blue (left panel). Scale bar = 50 um. The bottom 183 um of each villi were scored for alcian blue cells and 26-58 villi were scored in Msi1+/+ mice and 21-68 villi in Msi1-/- mice. (B) Data is presented as the average of all data samples +/- s.e.m. The average number of Goblet cells/villi in Msi1$^{+/+}$ jejunum was found to not statistically differ compared to Msi1$^{-/-}$ jejunum (p=0.772) as determined by student t-test (values <0.05 considered significant).**

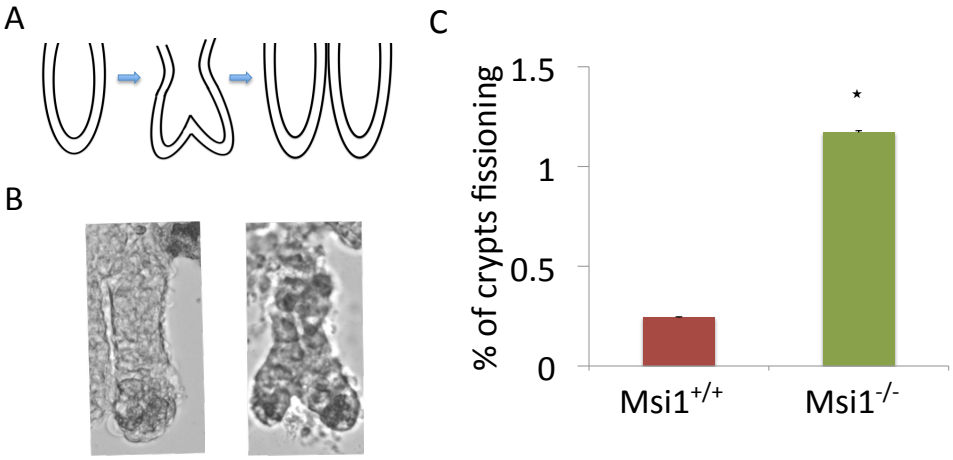

Figure 2.5. ***Elevation of Crypt fission in the small intestine of Msi1$^{-/-}$ mice.*** **(A) Schematic of the process of crypt fission. Fission is initiated when cypts reach a certain threshold of stem cells where crypts bifurcate along the bottom and eventually split into two crypts. (B) Representative images of crypts scored. Panel on the left is an image of a crypt not undergoing fission while the panel on the right shows a crypt undergoing fission. (C) Crypts were isolated from the small intestine via EDTA chelation and shaking and scored at 160x for fission. Data is presented as the average percent of crypts fissioning in the small intestine of 5 Msi1$^{+/+}$ mice and 3 Msi1$^{-/-}$ mice +/- the s.e.m. 364-736 crypts scored were scored/mouse in Msi1$^{+/+}$ mice and 364-736 crypts/mouse scored in Msi1$^{-/-}$ mice. There were a higher percent of crypts undergoing fission in Msi1$^{-/-}$ mice ($p = 0.0357$) compared to Msi1$^{+/+}$. P-values < 0.05 as calculated by the Mann-Whitney non-parametric test are considered significant.**

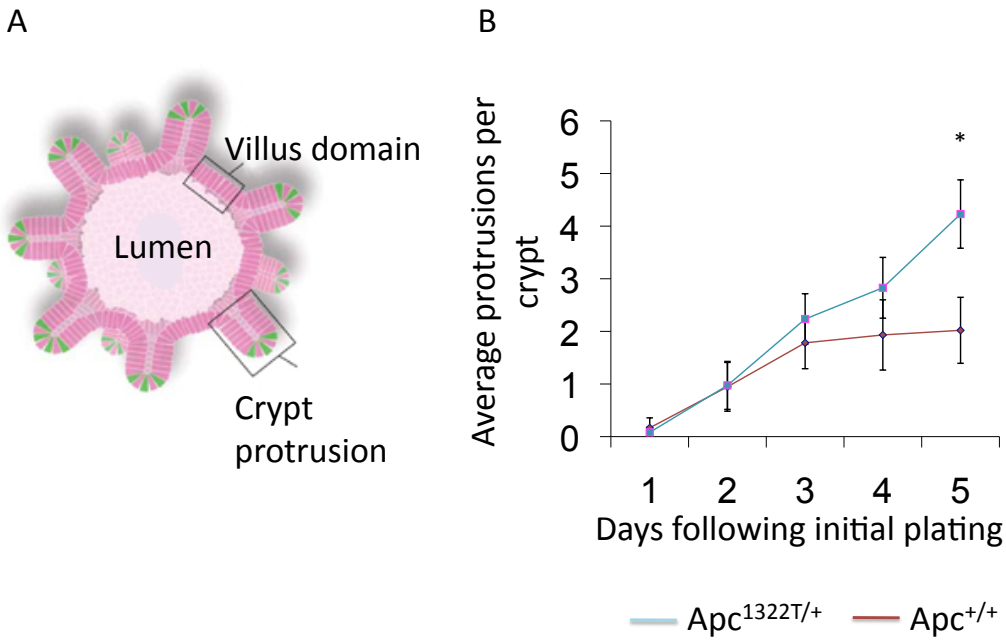

Figure 2.6. ***Crypt culture from*** **Apc$^{1322T/+}$** ***mice produce more protrusion than*** **Apc$^{+/+}$.** **(A) A schematic diagram of a crypt organoid adapted from Sato, T., et al. (2009)** ***Nature,*** **459 (7244), 262-5. Villus domains contain all differentiated cells and crypt protrusions contains stem cells. (B) To determine whether an** ***ex vivo*** **culture system would be an accurate measure of stemness, we cultured crypts from an Apc$^{1322T/+}$ and Apc$^{+/+}$ mouse. In agreement with previously published data, which show Apc$^{1322T/+}$ mice contain more stem cells in crypts, organoids from Apc$^{1322T/+}$ produce more protrusions. Results are presented as the average protrusion/organoid over a five day period and on day 5 Apc$^{1322T/+}$ had significantly more protrusions.**

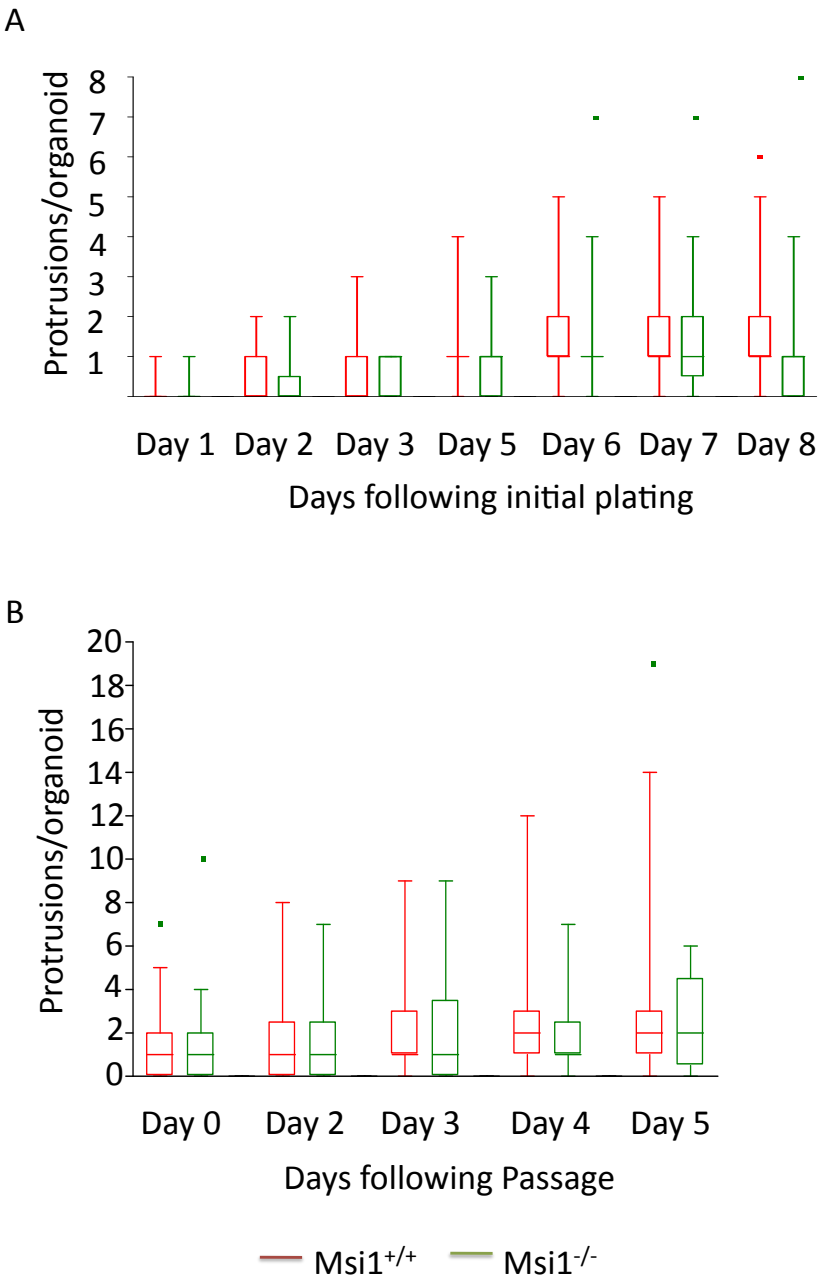

Figure 2.7. ***Msi1-/- organoids have less protrusions than Msi1+/+ organoids.*** **Crypts were isolated from one Msi1$^{+/+}$ and one Msi$^{-/-}$ mouse and grown in culture for a total of 15 days. Crypts would form organoids that would make protrusions that were then scored. (A) Results day 1 -8 after plating. Results are presented in a box-and-whisker plot, and outliers 4 standard deviations away from the mean were excluded but are displayed on graph. (B) Results after crypts were passaged displayed in box-and-whisker plot. Outliers 4 standard deviations away from the mean are excluded.**

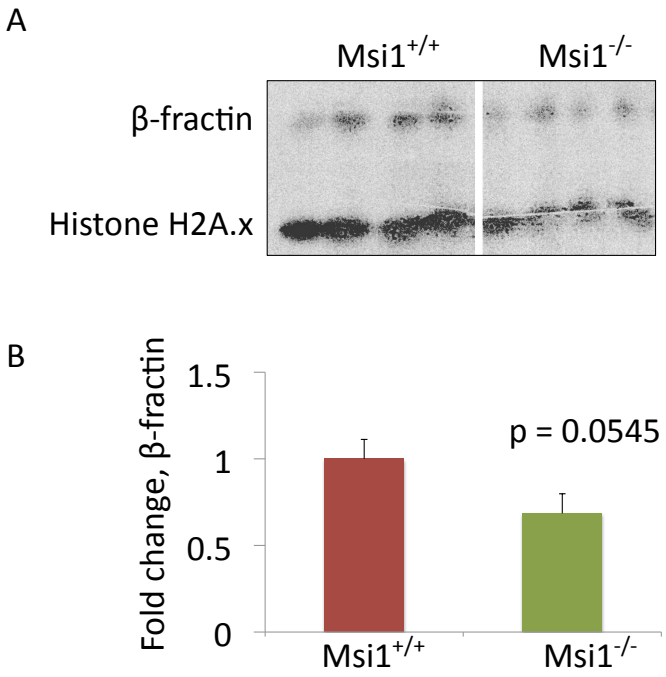

Figure 2.8. ***Apoptosis in the small intestine of Msi1$^{-/-}$ mice*****. (A) Representative blot showing protein samples from both mice genotypes. Protein was isolated from epithelial cells of the small intestines of 4 Msi1$^{+/+}$ and 7 Msi1$^{-/-}$ mice. (B) β-fractin protein levels were normalized to histone H2A.x, and are presented as average fold change relative to Msi1$^{+/+}$ mice +/- s.e.m. β-fractin levels were found to be lower in the small intestine of Msi1$^{-/-}$ mice, although it did not reach statistical significance (p= 0.0545). P-values < 0.05 as calculated by the Mann-Whitney non-parametric test are considered significant.**

Results: Colon

No significant change in Apc protein levels in the colon.

To see how loss of Msi1affects Apc protein levels, we performed immunoblot analysis using protein from the colons of $Msi1^{-/-}$ and $Msi1^{+/+}$ mice. We hypothesized that there would be an increase in Apc levels in colons from $Msi1^{-/-}$ mice. Our results showed that Apc levels were slightly elevated in colonic epithelial cells from $Msi^{-/-}$ mice, but not significantly so (Figure 2.9A and 2.9B).

No significant change in levels of Wnt target genes.

As in the small intestine, we looked at upregulated Wnt target genes, *c-Myc*, *axin-2*, and *cyclin-D1,* downregulated Wnt target gene *Hath1*, and *BTEB2* mRNA levels in the small intestine utilizing rt-PCR (Figure 2.10). *C-Myc*, *axin-2*, and *cyclin-D1* levels remained unchanged as did *Hath1* level. Interestingly, levels of BTEB2, a non-canonical Wnt target gene, were upregulated significantly. These results along with the finding that Apc protein levels are unaffected, suggest that the Msi-1/Apc feedback loop may not play an integral role in large intestinal homeostasis.

Proliferation in the colon of $Msi1^{-/-}$ mice is reduced.

Though we found no evidence linking Msi1 with Wnt signaling regulation in the colon, Msi1 likely has other functions in the colon. To examine functions of Msi1 in the colon, we first looked at the effects of Msi1 loss on proliferation. Again, large intestinal tissue was isolated from $Msi1^{-/-}$ mice and probed for Ki67, a proliferation marker. There was a significant decrease in the number of Ki67-positive cells per crypt in the colons of $Msi1^{-/-}$ mice (Figure 2.11A and 2.11B).

Crypt fission in the colon of $Msi1^{-/-}$ mice is reduced.

Finding that proliferation was reduced, we next examined crypt fission in the colons of $Msi1^{-/-}$ mice as well. It could be imagined that the level of proliferation would correlate with crypt fission. Along this line of reasoning, we hypothesized that fission would be reduced in the colons of Msi1-/- mice because proliferation was reduced. To test this, we isolated crypts from colon tissue and examined them for fissioning. We found the amount of crypt fissioning was significantly lower in $Msi1^{-/-}$ mice than $Msi1^{+/+}$ (Figure 2.12A and B).

Apoptosis in the colon of Msi1 -/- mice remains unchanged.

Because there was decreased proliferation and crypt fission in colons of $Msi1^{-/-}$ mice, we predicted that there would be a compensatory affect on apoptosis as well. We collected protein from the colon of $Msi1^{-/-}$ mice and examined β-fractin

levels via immunoblot. β-fractin levels remained unchanged in $Msi1^{-/-}$ as compared to $Msi1^{+/+}$ control mice (Figure 2.13).

Discussion

The goal of this study was to correlate predicted consequences of the Msi1/Apc double-negative feedback loop with phenotypes found in the colons of Msi1 knockout mice. In this set of experiments, our results were found largely to not be associated with results expected following disruption of the Apc/Msi1 double-negative feedback loop. First, there was not a significant increase in Apc protein level in colons from $Msi1^{-/-}$ mice. Second, the same three Wnt target genes, *cyclin-D1, c-myc, and axin-2* which are upregulated in canonical Wnt signaling, as well as Hath1 which is downregulated by canonical Wnt signaling were not differentially expressed in the colons of $Msi1^{-/-}$ and $Msi1^{+/+}$ mice. However, BTEB2 a non-canonical Wnt target was upregulated significantly in $Msi1^{-/-}$ mice. No previous reports have connected BTEB2 with Msi1 so further investigation will be needed to define this relationship. Our results support the idea that the Apc/Msi1 double-negative feedback loop does not play an integral role in homeostasis of the mouse colon and Msi1's function in other signaling pathways such as Notch may be more prominent in this tissue.

In support of the hypothesis that Msi1 and its association with Notch have a more prominent effect in the colon, proliferation and crypt fission were decreased in colons from $Msi1^{-/-}$ mice. Previously, it was shown that loss of Numb, a target of

translational inhibition of Msi1 and an inhibitor of the Notch pathway, causes proliferation in LS174T colon cancer cells (*25*). It is conceivable that in Msi1$^{-/-}$ mice, alleviation of Msi1 translational repression of Numb allows for repression of Notch signaling and a subsequent decrease in cell proliferation. Crypt fission, which has been thought to be linked to size of the crypt and stem cell number, would be expected to be reduced in these mice which is corroborated by our data.

No change was found in the levels of β-fractin, a protein cleaved during apoptosis, between the two genotypes. β-fractin has been shown to be a specific marker of apoptosis in different cells of the nervous system (*26*). However, it has not been tested in the intestine. Future studies should consider use of a different marker of apoptosis, such as cleaved caspase 3.

In summary, loss of Msi1 in the colon of mice, appears to play a role independent of the double-negative feedback loop between Apc and Msi1 that was established in cultured colon cells. Apc protein levels as well as canonical Wnt target genes were largely unaffected in colons of Msi1$^{-/-}$ mice. Cellular proliferation and crypt fission appeared significantly decreased in Msi1$^{-/-}$ mice, however, these phenotypes could be explained by the role of Msi1 in the Notch signaling pathway. Future studies investigating consequences of Apc/Msi1 regulation using this mouse model should focus on the small intestine and will ultimately clarify a role for Msi1/Apc regulation in the suppression of tumor formation.

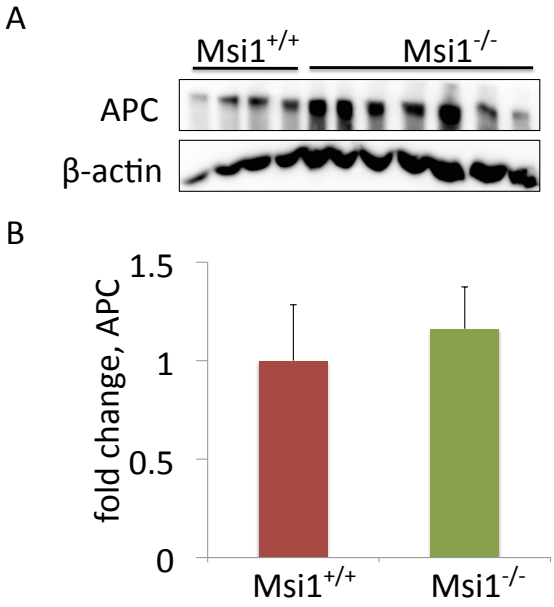

Figure 2.9. ***Apc protein levels in the colon*****. Apc protein levels were found to be unchanged in the colon of Msi1$^{-/-}$ mice compared to Msi1$^{+/+}$ (p=0.41958). (A) Representative blot of Apc protein levels in the colon. (B) Protein was isolated from epithelial cells of the colons of Msi1$^{+/+}$ and Msi1$^{-/-}$ mice. Apc relative band intensities from 4-10 mice were quantified, normalized to β-actin, and presented as average fold change relative compared to Msi1$^{+/+}$ mice +/- s.e.m. P-values < 0.05 as calculated by the Mann-Whitney non-parametric test are considered significant.**

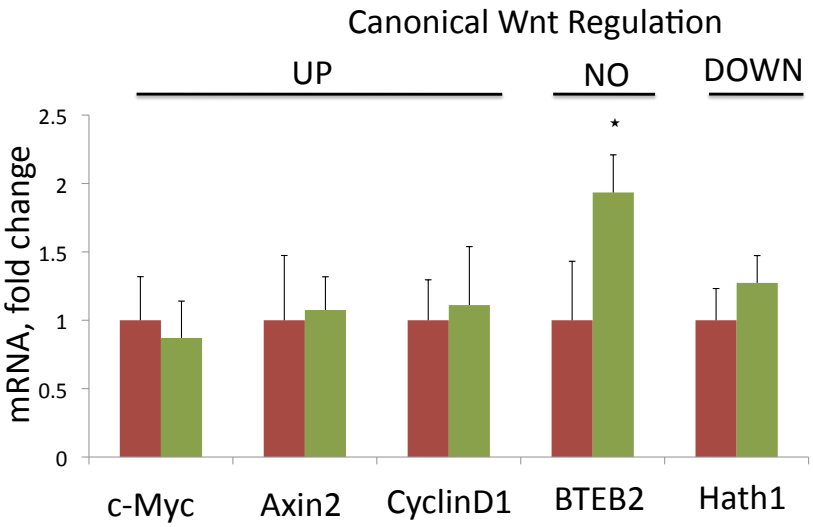

Figure 2.10. ***No significant difference in Wnt target genes in the colon of Msi1$^{-/-}$ mice.*** **Large intestinal epithelial cells were isolated from Msi1$^{+/+}$ mice and Msi1$^{-/-}$ mice. For each sample, mRNA levels were examined for three genes upregulated by Wnt signaling, *c-Myc*, *Axin2*, and *CyclinD1*, by reverse transcriptase-PCR. As controls, mRNA from one gene not regulated by Wnt signaling,*BTEB2*, and one gene downregulated by Wnt signaling, *Hath1*, were examined. Each gene was normalized to *HGPRT*, a housekeeping gene. The results from 5-10 mice are presented as the average mRNA fold change relative to Msi1$^{+/+}$ mice +/- s.e.m. P-values < 0.05 as calculated by the Mann-Whitney non-parametric test are considered significant and are indicated by an asterisk.**

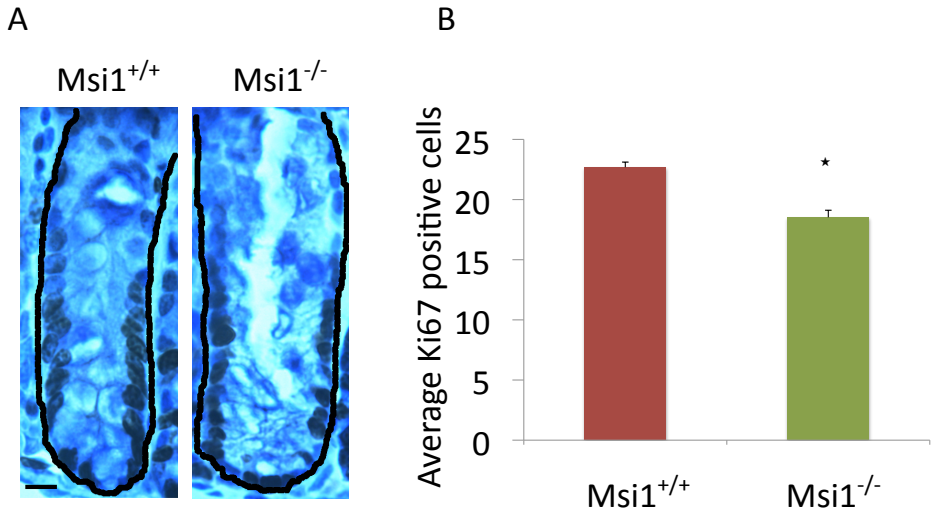

Figure 2.11. ***Proliferation in the colon of Msi1$^{-/-}$ mice is reduced compared to Msi1$^{+/+}$ mice.*** **(A) Representative images of cypts from Msi1$^{+/+}$ (left) and Msi1$^{-/-}$ (right) with the black line indicating crypt border. Scale bar = 10 um (left panel). (B) Samples were collected from 4 mice of each genotype and 27-100 crypts 75um-145um in length were scored per mouse. Data is presented as the average number of cells positive for proliferation marker Ki67 per crypt +/- s.e.m for all samples. Proliferation was decreased in Msi1$^{-/-}$ mice compared to Msi1$^{+/+}$ (p-value: 2.839E-08) as calculated by the student t-test. Significant values indicated by an asterisk.**

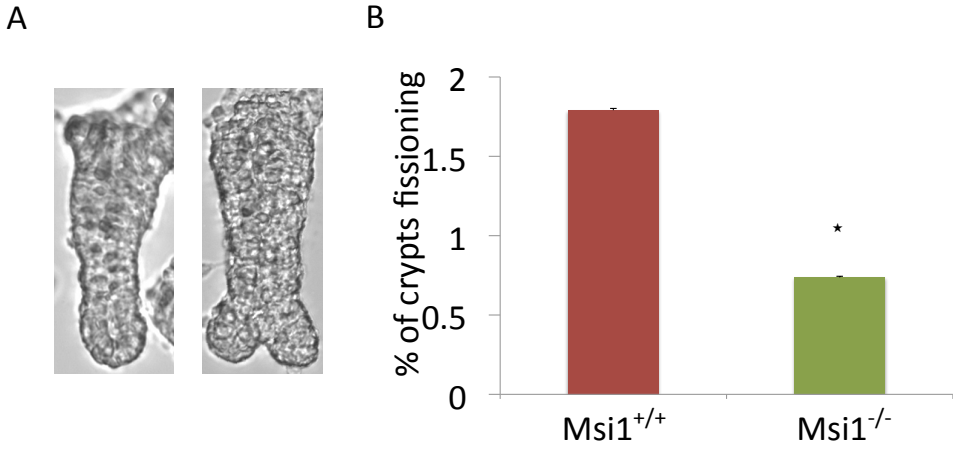

Figure 2.12. ***Decreased Crypt fission in the colon of Msi1$^{-/-}$ mice.*** **Crypts were isolated from the colon using EDTA chelation and shaking and scored at 160x for fission. (A) Representative image of a crypt not fissioning (panel on the left) and a crypt fissioning (panel on the right). (B) Data is presented as the average percent of crypts fissioning in the colon of 5 Msi1$^{+/+}$ mice and 4 Msi1$^{-/-}$ mice +/- the s.e.m. 364-736 crypts scored were scored/mouse in Msi1$^{+/+}$ mice and 523-826 crypts/mouse scored in Msi1$^{-/-}$ mice. There were a lower percent of crypts undergoing fission in Msi1$^{-/-}$ mice ($p = 0.0317$) compared to Msi1$^{+/+}$. P-values < 0.05 as calculated by the Mann-Whitney non-parametric test are considered significant. Significant values indicated by an asterisk.**

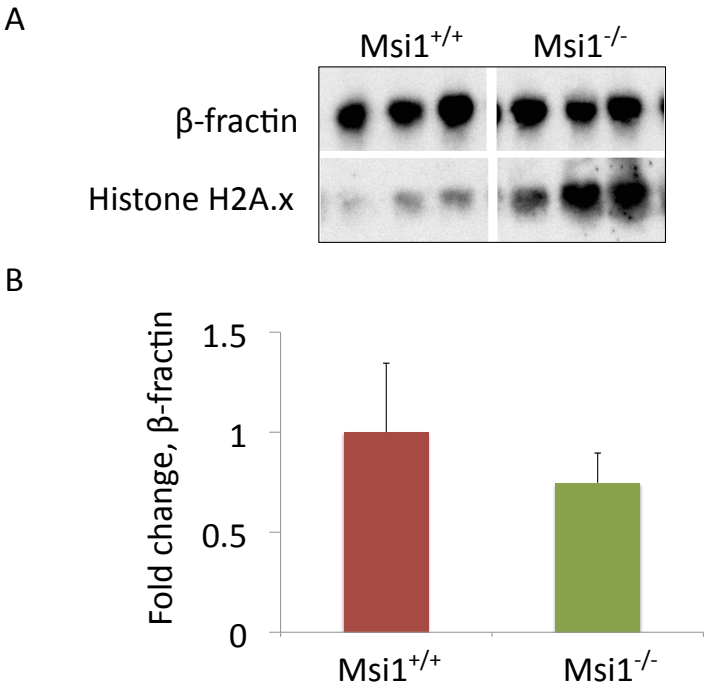

Figure 2.13. ***Apoptosis in the colon of Msi1$^{-/-}$ mice.*** **(A) Representative blot of β-fractin protein levels in the colon. Protein was isolated from epithelial cells of the colons of 4 Msi1$^{+/+}$ and 7 Msi1$^{-/-}$ mice. (B) β-fractin protein levels were normalized to histone H2A.x, and are presented as average fold change relative to Msi1$^{+/+}$ mice +/- s.e.m. β-fractin levels were found to be unchanged in the colon of Msi1$^{-/-}$ mice (p= 0.324). P-values < 0.05 as calculated by the Mann-Whitney non-parametric test are considered significant.**

Table 2.1: Summary of results in the Small Intestine and Colon

Phenotypes	Small Intestine	Colon
Wnt targets genes	Down-regulated	No change
APC protein levels	Up	No change
Proliferation	No change	Decreased
Goblet cell differentiation	No change	
Crypt fission	Increased	Decreased
Organoid Protrusions	Decreased	
Apoptosis	Down	No change

References

1. Leedham, S. J., Brittan, M., McDonald, S. A., and Wright, N. A. (2005) Intestinal stem cells, *J Cell Mol Med 9*, 11-24.
2. Barker, N., Ridgway, R. A., van Es, J. H., van de Wetering, M., Begthel, H., van den Born, M., Danenberg, E., Clarke, A. R., Sansom, O. J., and Clevers, H. (2009) Crypt stem cells as the cells-of-origin of intestinal cancer, *Nature 457*, 608-611.
3. Harada, N., Tamai, Y., Ishikawa, T., Sauer, B., Takaku, K., Oshima, M., and Taketo, M. M. (1999) Intestinal polyposis in mice with a dominant stable mutation of the beta-catenin gene, *EMBO J 18*, 5931-5942.
4. Sansom, O. J., Reed, K. R., Hayes, A. J., Ireland, H., Brinkmann, H., Newton, I. P., Batlle, E., Simon-Assmann, P., Clevers, H., Nathke, I. S., Clarke, A. R., and Winton, D. J. (2004) Loss of Apc in vivo immediately perturbs Wnt signaling, differentiation, and migration, *Genes Dev 18*, 1385-1390.
5. Potten, C. S., Booth, C., Tudor, G. L., Booth, D., Brady, G., Hurley, P., Ashton, G., Clarke, R., Sakakibara, S., and Okano, H. (2003) Identification of a putative intestinal stem cell and early lineage marker; musashi-1, *Differentiation 71*, 28-41.
6. Imai, T., Tokunaga, A., Yoshida, T., Hashimoto, M., Mikoshiba, K., Weinmaster, G., Nakafuku, M., and Okano, H. (2001) The neural RNA-binding protein Musashi1 translationally regulates mammalian numb gene expression by interacting with its mRNA, *Mol Cell Biol 21*, 3888-3900.
7. Battelli, C., Nikopoulos, G. N., Mitchell, J. G., and Verdi, J. M. (2006) The RNA-binding protein Musashi-1 regulates neural development through the translational repression of p21WAF-1, *Mol Cell Neurosci 31*, 85-96.
8. Spears, E., and Neufeld, K. L. (2011) Novel double-negative feedback loop between adenomatous polyposis coli and Musashi1 in colon epithelia, *J Biol Chem 286*, 4946-4950.
9. Rezza, A., Skah, S., Roche, C., Nadjar, J., Samarut, J., and Plateroti, M. (2010) The overexpression of the putative gut stem cell marker Musashi-1 induces tumorigenesis through Wnt and Notch activation, *J Cell Sci 123*, 3256-3265.
10. Sakakibara, S., Nakamura, Y., Yoshida, T., Shibata, S., Koike, M., Takano, H., Ueda, S., Uchiyama, Y., Noda, T., and Okano, H. (2002) RNA-binding protein Musashi family: roles for CNS stem cells and a subpopulation of ependymal cells revealed by targeted disruption and antisense ablation, *Proc Natl Acad Sci U S A 99*, 15194-15199.
11. Wang, Y., Azuma, Y., Friedman, D. B., Coffey, R. J., and Neufeld, K. L. (2009) Novel association of APC with intermediate filaments identified using a new versatile APC antibody, *BMC Cell Biol 10*, 75.
12. Zeineldin, M., Cunningham, J., McGuinness, W., Alltizer, P., Cowley, B., Blanchat, B., Xu, W., Pinson, D., and Neufeld, K. L. (2011) A knock-in mouse model reveals roles for nuclear Apc in cell proliferation, Wnt signal inhibition and tumor suppression, *Oncogene*.

13. Pinto, D., Gregorieff, A., Begthel, H., and Clevers, H. (2003) Canonical Wnt signals are essential for homeostasis of the intestinal epithelium, *Genes Dev 17*, 1709-1713.
14. Totafurno, J., Bjerknes, M., and Cheng, H. (1987) The crypt cycle. Crypt and villus production in the adult intestinal epithelium, *Biophys J 52*, 279-294.
15. Okano, H., Kawahara, H., Toriya, M., Nakao, K., Shibata, S., and Imai, T. (2005) Function of RNA-binding protein Musashi-1 in stem cells, *Exp Cell Res 306*, 349-356.
16. Ootani, A., Li, X., Sangiorgi, E., Ho, Q. T., Ueno, H., Toda, S., Sugihara, H., Fujimoto, K., Weissman, I. L., Capecchi, M. R., and Kuo, C. J. (2009) Sustained in vitro intestinal epithelial culture within a Wnt-dependent stem cell niche, *Nat Med 15*, 701-706.
17. Sato, T., Vries, R. G., Snippert, H. J., van de Wetering, M., Barker, N., Stange, D. E., van Es, J. H., Abo, A., Kujala, P., Peters, P. J., and Clevers, H. (2009) Single Lgr5 stem cells build crypt-villus structures in vitro without a mesenchymal niche, *Nature 459*, 262-265.
18. Lewis, A., Segditsas, S., Deheragoda, M., Pollard, P., Jeffery, R., Nye, E., Lockstone, H., Davis, H., Clark, S., Stamp, G., Poulsom, R., Wright, N., and Tomlinson, I. (2010) Severe polyposis in Apc(1322T) mice is associated with submaximal Wnt signalling and increased expression of the stem cell marker Lgr5, *Gut 59*, 1680-1686.
19. Morin, P. J., Vogelstein, B., and Kinzler, K. W. (1996) Apoptosis and APC in colorectal tumorigenesis, *Proc Natl Acad Sci U S A 93*, 7950-7954.
20. Leow, C. C., Romero, M. S., Ross, S., Polakis, P., and Gao, W. Q. (2004) Hath1, down-regulated in colon adenocarcinomas, inhibits proliferation and tumorigenesis of colon cancer cells, *Cancer Res 64*, 6050-6057.
21. Yang, Y., Zhu, R., Bai, J., Zhang, X., Tian, Y., Li, X., Peng, Z., He, Y., Chen, L., Ji, Q., Chen, W., Fang, D., and Wang, R. (2011) Numb modulates intestinal epithelial cells toward goblet cell phenotype by inhibiting the Notch signaling pathway, *Exp Cell Res 317*, 1640-1648.
22. Shi, F., Cheng, Y. F., Wang, X. L., and Edge, A. S. (2010) Beta-catenin up-regulates Atoh1 expression in neural progenitor cells by interaction with an Atoh1 3' enhancer, *J Biol Chem 285*, 392-400.
23. Zheng, X., Tsuchiya, K., Okamoto, R., Iwasaki, M., Kano, Y., Sakamoto, N., Nakamura, T., and Watanabe, M. (2011) Suppression of hath1 gene expression directly regulated by hes1 via notch signaling is associated with goblet cell depletion in ulcerative colitis, *Inflamm Bowel Dis*.
24. Sureban, S. M., May, R., George, R. J., Dieckgraefe, B. K., McLeod, H. L., Ramalingam, S., Bishnupuri, K. S., Natarajan, G., Anant, S., and Houchen, C. W. (2008) Knockdown of RNA binding protein musashi-1 leads to tumor regression in vivo, *Gastroenterology 134*, 1448-1458.
25. Pece, S., Serresi, M., Santolini, E., Capra, M., Hulleman, E., Galimberti, V., Zurrida, S., Maisonneuve, P., Viale, G., and Di Fiore, P. P. (2004) Loss of negative regulation by Numb over Notch is relevant to human breast carcinogenesis, *J Cell Biol 167*, 215-221.

26. Schulz, R., Vogel, T., Mashima, T., Tsuruo, T., and Krieglstein, K. (2009) Involvement of Fractin in TGF-beta-induced apoptosis in oligodendroglial progenitor cells, *Glia 57*, 1619-1629.

Chapter 3

Discussion

Summary of Results

APC and its canonical role as a negative regulator of Wnt signaling has been extensively studied. Loss of APC has been shown to be a critical initiating step in colorectal tumorigenesis and treatment strategies that can be devised to compensate for the loss of this critical gatekeeper gene are needed. Our lab previously showed that translation of APC is inhibited by MSI1. MSI1 also has been shown to play a crucial role in maintaining stemness characteristics in progenitor cell populations through activation of both the Wnt and Notch signaling pathways (*1, 2*) and is upregulated in colorectal cancer in both mouse models and humans (*3, 4*). Our lab and another lab, has shown MSI1 to be a Wnt target (*1, 5, 6*) and expression of MSI1 inhibits APC expression, promoting Wnt signaling. The implications of disruption of this double negative feedback regulation are important considerations before utilizing this regulatory mechanism as a potential target for treatment in tissues that lack functional APC. The work in this thesis has focused on consequent changes in intestinal tissue homeostasis that result from germ-line knock-out of Msi1 in mice, with particular emphasis on proliferation and differentiation. We have shown that in the small intestine, proliferation and differentiation are unaltered in mice lacking Msi1. However, Apc protein levels were seen to increase and Wnt target genes, especially those linked to proliferation, Cyclin D1 and c-Myc were seen to decrease. These results suggest that at the molecular level, the Apc-Msi1 double-negative feedback loop was disrupted. Fission events and crypt protrusion growth were also affected, though in different ways and apoptosis was decreased. In the large intestine, Apc and Wnt target genes were not

affected by Msi1 knockout, indicating that perhaps in this tissue Msi1 plays a more prominent role in other signaling pathways such as Notch. Proliferation was found to significantly decrease and apoptosis remained unaffected.

Disruption of the double-negative feedback loop between Apc and Msi1 should have an impact on different cellular phenotypes depending on how this regulation is altered. In colorectal cancer for instance, with loss of functional APC, Msi1, as a Wnt target gene would be highly expressed and cellular proliferation and a stem-like state would be favored. Evidence supporting this includes that Msi1 levels as well as proliferation were shown to be elevated in small intestine upon conditional knockout of Apc in a mouse model (*4*). Msi1 overexpression has also been directly linked to high proliferation and expansion of progenitor populations (*1*). Also, Lgr5+ progenitor cells, a progenitor where Msi1 is expressed, were shown to be able to cause adenomas upon conditional loss of APC (*7*). At the other extreme, where Msi1 is absent from the feedback loop, APC levels should be high and phenotypes associated with differentiation and quiescence would be favored.

However, because our data indicate that phenotypes related to proliferation and differentiation remained unaffected in mouse small intestine, the critical nature of this feedback loop may only be apparent upon cellular stress. Msi1 knockout mice develop neural phenotypes but otherwise are unaffected by germ-line knockout of this gene (*8*). If Msi1 played a critical role in intestinal homeostasis, a more severe phenotype would be expected in the intestine. Also, Msi1 knock-down has previously been shown to only elicit an effect in colon cancer cell lines and xenografts (*9*). And, Msi1 was found to be tumorigenic in normal intestinal

epithelia cells only upon high over-expression (*1*). Therefore, phenotypes related to loss of Msi1 in the intestine may depend upon induction of stress.

Alternatively, effects of the Apc / Msi1 double-negative feedback regulation may be more integral in the stem-cell compartment of the intestine, and the method of using the whole intestine to dissect out phenotypes related to this feedback loop may not be sensitive enough. Msi1 expression is restricted mainly to the progenitor compartment (*10*), therefore the APC-Msi1 regulation is probably more critical in this compartment. By isolating epithelial cells from the whole intestine, the effects of APC-Msi1 regulation may be diluted.

Msi1 plays an important role in signaling pathways integral to the maintenance of intestinal epithelia. Msi1 plays a role in activating Notch signaling through inhibition of m-Numb (*11*). Along with Wnt signaling, Notch is involved in promoting proliferation in the progenitor compartment and allowing for differentiation between absorptive and secretory lineages further up the crypt (*12*). Msi1 plays a role in activating Wnt signaling, another pathway needed to promote stemness in progenitors, through inhibition of Apc (*6*). Though these two pathways are both important and Msi1 was found to be an activator of both, the activation of these pathways by Msi1 are two independent events (*1*). Therefore, it is conceivable that both pathways may have different levels of importance in different tissues. In the large intestine, mucus producing cells are especially important for facilitating the removal of dehydrated waste and are at increased numbers compared with the small intestine. Notch signaling has been shown to be integral for goblet cell fate determination (*13-15*). Activation of Notch has been shown to

deplete goblet cells (*15*); inhibition of Notch promotes goblet cell differentiation (*13, 14*). As a regulator of Notch, Msi1 therefore may have a more prominent role in helping to establish secretory cell fate in the large intestine and thereby its role in Wnt signaling may be overshadowed. In this study, scoring differentiation of goblet cells was unsuccessful. Alcian blue staining, which was used previously to mark goblet cells, did not yield specific staining. Future studies will be required to distinguish the roles played by Msi1 in both tissues in order to link cellular phenotypes with different signaling pathways.

Future Studies

My studies have highlighted some of the cellular phenotypes associated with germ-line knockout of Msi1 and the effects of this knockout on Wnt signaling in the intestine. However, there are still studies that need to be undertaken to further connect Msi1 and Apc in the small intestine and the implications of this negative feedback loop on intestinal homeostasis.

I would propose to further develop the project that I have presented in this dissertation by expanding studies of the various phenotypes presented here. First, I only present data for differentiation of one cell type of the secretory lineage, Goblet cells, in the small intestine. It has been shown that Msi1 expression in LS174T cells can suppress paneth cell specific markers (*16*). However, this study also showed that markers related to other cell types were unaffected by Msi1 expression. Therefore, Msi1 knockout may have an effect on paneth cell differentiation to a

higher degree than other cell types. To compliment the Ki-67 analysis, injecting mice with BrdU and then staining tissue to identify positive cells would be a secondary way to show proliferation. Because loss of Apc and overexpression of Msi1 both have shown to be connected to increases in proliferation and our study currently shows no difference in proliferation in the small intestine, a secondary method would allow for more confidence in the data presented. Along with proliferation, apoptosis should be assessed by a secondary method. Commonly, apoptosis is assessed by immunohistochemistry for activated caspase 3 and this method may detect apoptosis more directly. Also, a direct method to assess stem cell numbers in the crypt needs to be established. Our methods of scoring organoid protrusions as well as fission to determine stem cell number are indirect and need to be corroborated with direct evidence regarding stem cell number. Though staining for specific stem cell markers was unsuccessful in the current study, other methods are present to assess stem cell number. For instance, real-time quantitative PCR could be performed to assess the amount of transcript for either Lgr5 or Bmi1 both of which mark stem cell populations in the intestine. Finally, a direct method to establish involvement of the Apc/Msi1 negative feedback mechanism with Wnt and Notch signaling in the intestine should be pursued. For the small intestine, to determine whether Wnt signaling is activated, nuclear localization of β-catenin could be compared between $Msi1^{-/-}$ and $Msi1^{+/+}$ mice. Reduced levels of nuclear β-catenin would indicate less Wnt signaling. In the large intestine, reduction of Notch target, Hes1, would show that loss of Msi1 affected Notch signaling.

Along with further examining the double-negative feedback loop in tissue of $Msi1^{-/-}$ mice, it would be critical to identify whether this double-negative feedback loop is important in cancerous tissue. Specifically, does manipulation of this feedback loop by removing Msi1 from the tissue allow for reduction of tumors? To this end, we are currently breeding $Msi1^{-/-}$ mice with $Apc^{Min/+}$ mice. We hypothesize that these double-mutant mice will have a reduced tumor burden as compared to the $Apc^{Min/+}$ mice.

To examine the effects of Msi1 and Apc in cancerous tissue at the molecular level, the crypt culturing system could be used. $Apc^{Min/+}$ or $Apc^{1322T/+}$ crypts could be grown and knock-down of Msi1 using siRNA could be employed. The examination of effects in $Apc^{1322T/+}$ crypts upon loss of Msi1 would be particularly pertinent to the role of Msi1 in stem cells because in this mouse model the stem cell number is increased (*17*). If Msi1 knockdown had an effect on reducing stemness of these organoids, this would lend support for its possible use as a target for cancer therapy.

Finally, it would be interesting to determine whether other mechanisms contributed to the reduction of proliferation in the colon aside from Wnt signaling or Notch signaling. Msi1 has been shown to downregulate levels of $p21^{waf1}$, a repressor of cyclin-dependent kinases, and overexpression of Msi1 was shown to allow for enhanced S-phase entry (*18*). So, knockout of Msi1 may lead to an upregulation of $p21^{waf1}$, which would allow for the decrease seen in the proliferation in the colon. So, Msi1's role in cell-cycle regulation would be an avenue of research to explore.

In summary, the Apc-Msi1 double negative feedback loop was examined in the intestinal tissue of $Msi1^{-/-}$ mice. Data from the small intestine fit our hypothesis that disruption of this regulatory mechanism would reduce Wnt signaling. However, some phenotypes associated with Wnt signaling were unaffected. In the large intestine, loss of Msi1 had no apparent affect on Apc levels or most phenotypes associated with Wnt signaling. Future studies will need to further examine the importance of this regulatory mechanism in tissue and determine whether this regulation is important in cancerous tissues. With further understanding, Msi1, via its role in this feedback loop, may be an important target for future colon cancer therapy.

References

1. Rezza, A., Skah, S., Roche, C., Nadjar, J., Samarut, J., and Plateroti, M. (2010) The overexpression of the putative gut stem cell marker Musashi-1 induces tumorigenesis through Wnt and Notch activation, J Cell Sci 123, 3256-3265.
2. Wang, X. Y., Yin, Y., Yuan, H., Sakamaki, T., Okano, H., and Glazer, R. I. (2008) Musashi1 modulates mammary progenitor cell expansion through proliferin-mediated activation of the Wnt and Notch pathways, Mol Cell Biol 28, 3589-3599.
3. Li, D., Peng, X., Yan, D., Tang, H., Huang, F., Yang, Y., and Peng, Z. (2011) Msi-1 is a predictor of survival and a novel therapeutic target in colon cancer, Ann Surg Oncol 18, 2074-2083.
4. Sansom, O. J., Reed, K. R., Hayes, A. J., Ireland, H., Brinkmann, H., Newton, I. P., Batlle, E., Simon-Assmann, P., Clevers, H., Nathke, I. S., Clarke, A. R., and Winton, D. J. (2004) Loss of Apc in vivo immediately perturbs Wnt signaling, differentiation, and migration, Genes Dev 18, 1385-1390.
5. Shi, F., Cheng, Y. F., Wang, X. L., and Edge, A. S. (2010) Beta-catenin up-regulates Atoh1 expression in neural progenitor cells by interaction with an Atoh1 3' enhancer, J Biol Chem 285, 392-400.

6. Spears, E., and Neufeld, K. L. (2011) Novel double-negative feedback loop between adenomatous polyposis coli and Musashi1 in colon epithelia, J Biol Chem 286, 4946-4950.
7. Barker, N., Ridgway, R. A., van Es, J. H., van de Wetering, M., Begthel, H., van den Born, M., Danenberg, E., Clarke, A. R., Sansom, O. J., and Clevers, H. (2009) Crypt stem cells as the cells-of-origin of intestinal cancer, Nature 457, 608-611.
8. Sakakibara, S., Nakamura, Y., Yoshida, T., Shibata, S., Koike, M., Takano, H., Ueda, S., Uchiyama, Y., Noda, T., and Okano, H. (2002) RNA-binding protein Musashi family: roles for CNS stem cells and a subpopulation of ependymal cells revealed by targeted disruption and antisense ablation, Proc Natl Acad Sci U S A 99, 15194-15199.
9. Sureban, S. M., May, R., George, R. J., Dieckgraefe, B. K., McLeod, H. L., Ramalingam, S., Bishnupuri, K. S., Natarajan, G., Anant, S., and Houchen, C. W. (2008) Knockdown of RNA binding protein musashi-1 leads to tumor regression in vivo, Gastroenterology 134, 1448-1458.
10. Potten, C. S., Booth, C., Tudor, G. L., Booth, D., Brady, G., Hurley, P., Ashton, G., Clarke, R., Sakakibara, S., and Okano, H. (2003) Identification of a putative intestinal stem cell and early lineage marker; musashi-1, Differentiation 71, 28-41.
11. Imai, T., Tokunaga, A., Yoshida, T., Hashimoto, M., Mikoshiba, K., Weinmaster, G., Nakafuku, M., and Okano, H. (2001) The neural RNA-binding protein Musashi1 translationally regulates mammalian numb gene expression by interacting with its mRNA, Mol Cell Biol 21, 3888-3900.
12. Medema, J. P., and Vermeulen, L. (2011) Microenvironmental regulation of stem cells in intestinal homeostasis and cancer, Nature 474, 318-326.
13. Fre, S., Hannezo, E., Sale, S., Huyghe, M., Lafkas, D., Kissel, H., Louvi, A., Greve, J., Louvard, D., and Artavanis-Tsakonas, S. (2011) Notch lineages and activity in intestinal stem cells determined by a new set of knock-in mice, PLoS One 6, e25785.
14. Fre, S., Huyghe, M., Mourikis, P., Robine, S., Louvard, D., and Artavanis-Tsakonas, S. (2005) Notch signals control the fate of immature progenitor cells in the intestine, Nature 435, 964-968.
15. van Es, J. H., van Gijn, M. E., Riccio, O., van den Born, M., Vooijs, M., Begthel, H., Cozijnsen, M., Robine, S., Winton, D. J., Radtke, F., and Clevers, H. (2005) Notch/gamma-secretase inhibition turns proliferative cells in intestinal crypts and adenomas into goblet cells, Nature 435, 959-963.
16. Murayama, M., Okamoto, R., Tsuchiya, K., Akiyama, J., Nakamura, T., Sakamoto, N., Kanai, T., and Watanabe, M. (2009) Musashi-1 suppresses expression of Paneth cell-specific genes in human intestinal epithelial cells, J Gastroenterol 44, 173-182.
17. Lewis, A., Segditsas, S., Deheragoda, M., Pollard, P., Jeffery, R., Nye, E., Lockstone, H., Davis, H., Clark, S., Stamp, G., Poulsom, R., Wright, N., and Tomlinson, I. (2010) Severe polyposis in Apc(1322T) mice is associated with submaximal Wnt signalling and increased expression of the stem cell marker Lgr5, Gut 59, 1680-1686.

18. Battelli, C., Nikopoulos, G. N., Mitchell, J. G., and Verdi, J. M. (2006) The RNA-binding protein Musashi-1 regulates neural development through the translational repression of p21WAF-1, Mol Cell Neurosci 31, 85-96.

Appendix Chapter

Interaction of Endogenous Truncated APC and Topo IIα, Conditions for Co-immunoprecipitation of APC Domains APC with Topo IIα

Abstract

Adenomatous polyposis coli (APC) and topoisomerase IIα (topo IIα) have been shown by our lab to interact and have an influence on the G2/M transition in the cell cycle. However, only the central portion of the APC protein was examined for topo IIα interaction and whether other portions of the APC protein have an interaction with topo IIα remains unknown. Also, whether truncated APC in colon cancer will interact with topo IIα has yet to be tested. To further characterize interactions of APC and topo IIα, we introduced a nuclear localization signal onto APC domains that had not been previously examined because of their cytoplasmic localization and showed that these constructs successfully localize to the nucleus. However, binding interactions with topo IIα still need to be established. We also examined whether endogenous truncated APC found in HT29 cells interacted with topo IIα. We found that a truncation containing the M2 portion of APC does interact with topo IIα while a shorter truncation encompassing the N-terminal portion of APC does not show interaction with topo IIα. Through further characterization of topo IIα/APC interactions, more complete understanding of how these proteins work together to regulate the cell cycle can be achieved, ultimately determining if misregulation caused by truncated APC interacting with topo IIα contributes to the pathogenesis of colorectal cancer.

Introduction

Topoisomerase IIα (topo IIα), an enzyme integral to cell cycle progression, is over-expressed in many colorectal cancers (*1*). The normal function of topo IIα is to allow for detanglement of DNA during cell replication, transcription, and metaphase in actively growing cells (*2*), and topo IIα expression is normally restricted to the proliferative zone in the colon(*1*). Topo IIα is involved in DNA decatenation by introducing a transient double strand break in the DNA and then undergoing a conformational change that allows for passage of a second DNA to relieve entanglement(*2*). If topo IIα is not functioning properly, then cells halt at the G2/M decatenation checkpoint (*3*).

APC has also been shown to play an active role in the cell cycle. A previous study showed that when APC was ectopically expressed in a colon cancer cell line with mutant APC, cells arrested at G1 due to repression of Wnt target Cyclin D1(*4*). Also, zinc chloride treatment of a colon cancer cell line expressing full-length APC caused arrest in the G2/M phase of the cell cycle (*5*). Previously, our lab showed that APC present in the nucleus allowed for G2/M arrest by interacting with topo IIα. Exogenously expressed pieces of APC, M2-APC (amino acids 999-1326) and M3-APC (amino acids 1327-2058), interacted with topo IIα and lead to altered nuclear morphology, accumulation of cells in the G2 phase of the cell cycle, and altered decatenation activity (*6, 7*). However, whether the other portions of the APC protein, including the, NT, M1, and CT fragments, would interact with topo IIα and whether these interactions would affect the cell cycle remained unknown. Also, whether topo IIα interacts with truncated APC expressed in colon cancer cells was

unknown. Here, we show in HT29 cells that the longer endogenous APC truncated protein, amino acids 1-1555 which contains the M2 portion of APC, interacts with topo IIα while the shorter truncation in the same cell line, which includes only the N-terminal portion of APC, does not. Also, we show that when NT, M1, and CT fragments are fused to a nuclear localization signal, they can successfully translocate into the nucleus. The interaction of these APC fragments with topo IIα still needs to be investigated. Finally, a list of procedures tested while optimizing the co-immunoprecipitation of NLS-APC fragments is provided.

Materials and Methods

Cell Culture.

HCT116βw cells were provided by Dr. Bert Vogelstein and grown in McCoy's 5A with 10% fetal bovine serum. HT29 cells were purchased from ATCC and were grown in McCoy's 5A with 10% fetal bovine serum.

Cloning of NLS into APC expression constructs.

Expression constructs for APC fragments fused to GFP, NT-APC, M1-APC, M2-APC, M3-APC, CT-APC**,** were provided by Dr. Naoki Watanabe and described in (*8*). The nuclear localization signal from SV40 virus large T antigen was cloned upstream of the APC gene using the following primers: upstream: 5' TGC GGA GGA TGC CCA AAA AAG AAG A 3', downstream: 5' TCG ACG TCT ACC TTT CTC TTC TTT 3'.

Transfection.

HCT116 β/w cells at 50% confluence were transfected with 16 μg of NLS APC expression plasmids or GFP plasmid with GeneExpresso reagent (Lab Supply Mall) at a ratio of 1 μg DNA : 3.5 μL of reagent in 10 cm cell culture dishes. Transfection reagent was prepared by adding GeneExpresso/DNA solution to McCoy's 5A / 10% fetal bovine serum and then added to cells. Cells were grown for 48 hours following transfection before harvesting for protein analysis.

Coimmunoprecipitation of Endogenous truncated APC and topo IIα.

Immunoprecipitation was performed using a modified protocol from Invitrogen Dynabeads. Cells at 90% confluence were lysed in lysis buffer (50 mM Tris pH 7.5, 0.1% NP40, 100 mM NaCl, 1 mM MgCl2, 5 mM EDTA, 1:7 Roche EDTA-free (cat. no. 04693159001) protease inhibitor, 1:100 Halt phosphatase inhibitor (cat no. 78420) in 1x PBS) on ice for 5 minutes. The entire procedure was performed at 4°C. Cell lysates were filtered twice by passing lysate through a QIAshredder (Qiagen cat. no. 79654) and centrifuging at 9300 g to rupture cells and shred DNA. Antibodies including, 4 μg APC-M2 (Wang et al. 2009) and 4 μg rabbit IgG (Sigma) were pre-incubated with protein A magnetic Dynabeads (Invitrogen) for 10 minutes. One milligram of soluble lysate was added to antibody saturated Dynabeads and incubated at 2 hours with rotation. Supernatant was removed from beads and added to beads pre-incubated with 50 μg of ALI1228 antibody (Chemicon cat. no. MAB3785) specific for the N-terminal portion of APC. This reaction was allowed to incubate for 2 hours with rotation. In order to remove immunoprecipitated protein,

beads were subjected to two washes of PBS containing protease and phosphatase inhibitors followed by heating at 95°C in 5x sample buffer to dissociate protein from the beads. All samples were stored at -80°C until further use. See protocol below for a more detailed description of procedure.

Invitrogen Protocol with modifications

Solutions needed:

1. Lysis buffer:

   50 mM Tris pH 7.5, 0.1% NP40, 100 mM NaCl, 1 mM MgCl2, 5 mM EDTA, 1:7 Roche protease inhibitor, 1:100 Halt phosphatase inhibitor in 1x PBS
2. 0.02% Tween 20 in PBS
3. PBS (with protease and phosphatase inhibitor):

   1x PBS with1:7 Roche protease inhibitor, 1:100 Halt phosphatase inhibitor added.
4. 5x SDS loading buffer (see protein analysis Results for list of components).

Preparation of Protein A Dynabeads (Invitrogen cat. no. 10002D)

1. resuspend Dynabeads by flicking container.
2. transfer 50 μL Dynabeads to microfuge tube.
3. place tube on magnet to separate the beads from the solution, and remove the supernatant.
4. removed tube from magnet.

Binding of Antibody

5. add antibody to 200 µL PBS with 0.02% Tween 20.
6. Incubate with rotator 10 min.
7. Place tube on magnet and remove supernatant – supernatant may be kept for further analysis.
8. Remove tube from magnet and resuspend beads-antibody complex in 200 µL PBS with Tween 20.

Preparation of Cell lysate (Anna Wang's adapted protocol)

Procedure performed on ice or at 4°C

1. Add 1 mL lysis buffer to cells both HCT116 cells and HT29 cells grown to 80-90% confluence and incubate 5 min.
2. Pass sample through Qiashreder filter in microfuge tube, spin down 10,000 rpm, 2 min, resuspend, repeated twice.
3. Resuspend and collect 65 µL sample and label whole cell lysate.
4. spin down samples 10,600 rpm, 20 min. to pellet insoluble material.
5. remove supernatant into separate microfuge tube, keep pellet and label insoluble.
6. read protein concentration of supernatant (soluble fraction) on nanodrop OD280.
7. collect 65 µL sample from soluble fraction – label SL (soluble lysate).

Immunoprecipitation

8. put beads on magnet, remove supernatant and discard, remove beads from magnet.
9. add 1 mg of soluble fraction protein to beads and pipette up and down to resuspend – (calculation: 1mg/concentration of soluble lysate = volume of soluble fraction to add to beads in mL)
10. incubate 2 hours on rotator 4C
11. place tubes on magnet and transfer 65 µL of supernatant to new microfuge tube – label supernatant, discard extra supernatant
12. Wash dynabeads-antibody-antigen complex three times using 200 µL of PBS with protease and phosphatase inhibitors for each wash. Separate on the magnet between each wash, remove supernatant and resuspend by gentle pipeting.
13. Resuspend Dynabeads-antibody-antigen complex in 100 µL PBS and transfer bead suspension to a clean tube.
14. Put tube on magnet, remove supernatant, add 65 µL of PBS with protease and phosphatase inhibitors and 35 µL of SDS loading buffer.
15. Add 35 µL SDS loading buffer to all samples.
16. Heat all samples 5 min, 100°C.
17. Put tubes on magnet, remove supernatant to new tubes – label PD (pull-down), discard beads.
18. Vortex all samples 30 seconds.
19. Heat all samples 5 minutes, 100°C.

20. Vortex briefly, store at -80°C

Protein analysis for NLS-APC-GFP transfected constructs

Primary antibody used for immunoprecipitation was 4 μg of rabbit anti-GFP (Invitrogen) for all experimental conditions, unless otherwise stated. Modified Invitrogen protocol was used for all conditions unless otherwise stated.

Procedure1: Covalent conjugation of beads to antibody followed by IP:

Protein A dynabeads were washed twice with 1x PBS and antibody was incubated for 2 hours with the beads at room temperature. Beads conjugated to antibody were then washed twice with 0.2M triethanol amine pH 8.0. One mg of DMP was added and solution was immediately rotated for 15 minutes. 100 μL of 1M Tris pH 8.0 was added to the solution and the solution was rotated for 2 hours. The beads were washed twice with 1x PBS, then washed with 1/10x PBS, then 1 mL of 0.2M Glycine pH 2 twice, followed by PBS-T (1x PBS with 10mM Tris pH 8) three times.

Preparation of cell lysate and immunoprecipitation were done as above at 4°C. Following immunoprecipitation, beads were washed with cell lysis buffer twice for 15 minutes each followed by two washes with PBS 15 minutes each and protein was removed from beads as described above.

Procedure 2: Use of Invitrogen protocol with modifications

Modified Invitrogen protocol above was used.

Procedure 3: Use of lithium chloride or lysis buffer washes to remove non-specific binding from the beads

After immunoprecipitation with cell lysate, beads were divided in half and one set of beads was washed twice with 500 mM lithium chloride the other set was washed once with lysis buffer followed by a wash with 500 mM lithium chloride. Protein was removed from beads as above.

Procedure 4: Blocking the antibody-complexed beads with 5% gelatin.

After binding of beads to antibody, 5% gelatin was added to the antibody-complexed beads and incubated for 30 minutes to block antibody-complexed beads. The rest of the procedure was repeated as above.

Procedure 5: Use of a different GFP antibody

4 μg of The GFP antibody (rabbit anti-GFP, GeneScript cat. no. A017045) was incubated with the beads and the rest of the procedure was repeated as above.

Procedure 6: Use of DNase to remove DNA contamination

Following immunoprecipitation, beads were incubated in 5U DNase for 15 minutes at room temperature. The beads were then washed as described above and rest of procedure was followed.

Procedure 7: Pre-clearing the lysate

Modified Invitrogen protocol was used. In order to pre-clear the cell lysate, 10 mg of rabbit IgG antibody were added to the beads and incubated for 10 minutes. The cell lysate was incubated with IgG-beads for 2 hours at 4°C. The beads were removed, and the immunoprecipitation experiment was performed as above.

Immunoblot analysis

Immunoblots for coimmunoprecipitation of endogenous APC and topo IIα were blocked in 5% milk TBS-T and were probed with the following antibodies: rabbit anti-human topo IIα antibody (Azuma lab) 1:1000, APC-M2 1:3000, ALI12-28 1:100. Secondary antibodies used included: horseradish peroxidase goat anti-rabbit IgG (Bio-Rad cat. No. 172-1019) and HRP-rabbit anti-mouse IgGγ (Zymed cat. no. 61-6020). Blots were developed using SuperSignal West Femto Maximum Sensitivity Substrate (Pierce) and a Kodak Image Station 4000R. Experiment was repeated on three separate occasions with the same results.

Immunoblot for coimmunoprecipitation of APC constructs and topo IIα was performed as above and blots were probed with the following primary antibodies: Rabbit anti-GFP (Invitrogen) 1:1000 and rabbit anti-human topo IIα antibody (Azuma lab) 1:1000. Secondary antibodies included: horseradish peroxidase goat anti-rabbit IgG (Bio-Rad cat. No. 172-1019) and cleanblot IP detection reagent (HP) (Thermo Scientific).

Imaging for Nuclear localization of APC.

Examination of subcellular localization of NLS-APC-GFP was performed using a Nikon Eclipse TE3000-U inverted microscope at 400x magnification and images were acquired using Volocity 4.3.3 imaging software.

Results

The N-terminal portion of APC does not interact with topoisomerase IIα.

Previously, our lab has shown that exogenously expressed central portions of APC referred to as APC-M2 and APC-M3, bind to topo IIα and regulate its activity (*6, 7*). Because M2 is maintained in the truncated APC found in many colorectal cancers, we wanted to determine if different endogenous APC truncations interacted with topo IIα. To this end, we used HT29 cells, a colorectal cancer cell line that expresses two endogenous truncated APC fragments (tAPC). $tAPC^{1555}$ contains the M2 portion of the protein and $tAPC^{853}$ lacks any previously shown Apc/topo IIα binding regions (Fig app. 1.1A). We hypothesized that $tAPC^{1555}$ would show an interaction with topo IIα in HT29 cells but did not know whether topo IIα could interact with $tAPC^{853}$. In order to determine whether these different truncations of APC bound to topo IIα, coimmunoprecipitation was performed using an antibody specific for the M2 portion of APC. This procedure allowed for the cell lysate to be immuno-depleted of $tAPC^{1555}$ leaving behind $tAPC^{853}$. $tAPC^{853}$ was then immunoprecipitated with an antibody specific for the N-terminal portion APC. Immunoblot analysis was performed to determine whether topo IIα coimmunoprecipitated with either APC truncation (Fig. app. 1.1B). As expected

based on our previous binding studies, tAPC^{1555} coimmunoprecipitated with topo IIα. Both truncations of APC precipitated with the M2 antibody, likely because they can form dimers via an N-terminal dimerization domain. Topo IIα did not co-precipitate with APC^{853}.

Methods attempted to coimmunoprecipitate NLS-NT-APC, NLS-M1-APC, and NLS-CT-APC with topo IIα.

Previously, our lab has shown that M2-APC and M3-APC localize to the nucleus and coimmunoprecipitates with topo IIα. However, expression of M2-APC and M3-APC had differential effects on the cells and topo IIα activity. These effects included altered nuclear morphology, extent of G2 cell cycle accumulation, decatenation activity of topo IIα, as well as the amount of topo IIα that was precipitated with each construct (*6, 7*). These observations led to the hypothesis that different portions of APC may interact with topo IIα in different ways. In order to test this hypothesis, the other APC-GFP constructs were examined for coimmunoprecipitation with topo IIα. These constructs had not been previously used for coimmunoprecipitation because they did not localize to the nucleus and therefore were not expected to interact with topo IIα. However, it had not been shown whether these APC domains, if they were to localize to the nucleus, could interact with topo IIα. To facilitate nuclear localization of these APC domains, we made constructs that express the NLS from Simian Virus 40 (SV40) large T antigen fused with the N-terminus of various APC fragments linked to green fluorescent protein (GFP) and transfected these constructs into HCT116 cells. Each APC domain

appeared to localize to the nucleus of live cells (fig app 1.2A). We also successfully immunoprecipitated these constructs from HCT116 cell lysates using a GFP antibody (fig app 1.2B). However, upon probing the blot for topo IIα, we found topo IIα precipitating with the GFP antibody in cells transfected with GFP alone. We also found full-length APC precipitating with GFP antibody in both cells transfected with GFP and M2-APC (fig app 1.2C).

These results lead to a series of experiments designed to reduce non-specific binding to the GFP antibody used to immunoprecipitate the APC domains from cell lysates. A summary of the methods used is listed in Appendix Table 1. All optimization strategies attempted still yielded non-specific binding in the coimmunoprecipitations so were not further pursued. First, an entirely new protocol from Invitrogen, was used with modifications for the immunoprecipitation. The original protocol (see Materials and Methods protein analysis for NLS-APC-GFP constructs procedure 1) covalently conjugated the GFP antibody to the magnetic beads and yielded non-specific binding. The Invitrogen protocol with modifications (see Materials and Methods protein analysis for NLS-APC-GFP constructs procedure 2) was used successfully in the previous experiment to precipitate endogenous APC from HT29 cell lysates but was unsuccessful when used for immunoprecipitation with the GFP antibody. Modifications were then made to the Invitrogen protocol. The first modification was to wash the beads following immunoprecipitation with lithium chloride or lysis buffer to detach non-specific materials adhering to the beads (see Materials and Methods protein analysis for NLS-APC-GFP constructs procedure 3). These washes are far more stringent than PBS but were still

unsuccessful at eliminating the non-specific binding to the GFP antibody. Next, 5% gelatin was used to block the GFP-conjugated beads (see Materials and Methods protein analysis for NLS-APC-GFP constructs procedure 4). The next modification included pre-clearing the lysate from the cells using an IgG antibody conjugated to beads in order to remove non-specific protein before the immunoprecipitation was performed (see Materials and Methods protein analysis for NLS-APC-GFP constructs procedure 5). Finally, removal of potential DNA contamination from the immunoprecipitated material was attempted (see Materials and Methods protein analysis for NLS-APC-GFP constructs procedure 6). This modification was attempted because topo IIα had been shown to non-specifically bind DNA but it was unsuccessful.

Discussion

APC has many other roles in the cell in addition to its role in regulation of canonical Wnt signaling. Namely, our lab showed that APC has a function in cell-cycle regulation via its interaction with topo IIα. Specifically, full-length endogenous APC was shown to coimmunoprecipitate with topo IIα and the M2 and M3 portions were shown to interact with topo IIα and affect topo IIα activity (*6, 7*). However, it was unknown whether truncated APC from colon cancer cell lines interacted with topo IIα and whether other portions of APC aside from the central portion could interact with topo IIα. We show here that a long endogenous truncation of APC containing the M2 portion of the protein coimmunoprecipitated with topo IIα. A shorter truncation containing only the N-terminal portion of the

protein did not coprecipitate with topo IIα. We also have introduced a nuclear localization signal into the NT-APC, M1-APC, and CT-APC expression constructs for future analysis of specific APC domains. This work suggests that longer forms of endogenous truncated APC do interact with topo IIα and that further work needs to be done to establish whether other portions of APC interact with topo IIα.

There are many avenues to be pursued with this project. One potential project would be to determine co-localization of the NLS-APC fragments with endogenous topo IIα using fluorescence microscopy and Förster resonance energy transfer (FRET) analysis as an alternative method to complement the immunoprecipitation results. Another pressing question is whether the interaction between topo IIα and truncated APC makes colorectal cancers more resistant to treatments with common chemotherapeutic reagents, such as etoposide, which acts as a topo IIα poison. In a colon cancer cell, if truncated APC binds to topo IIα and renders it inactive, then it would be expected that etoposide would be ineffective, since this class of topo IIα poisons depends on active topo IIα to kill cells. Colon cancers are commonly resistant to treatment with topo IIα poisons (*9*), and it would be interesting to determine whether truncated APC helps promote this resistance. If such a role for truncated APC is found, we envision developing small molecules to specifically block this interaction and potentially restore sensitivity to topo IIα poisons.

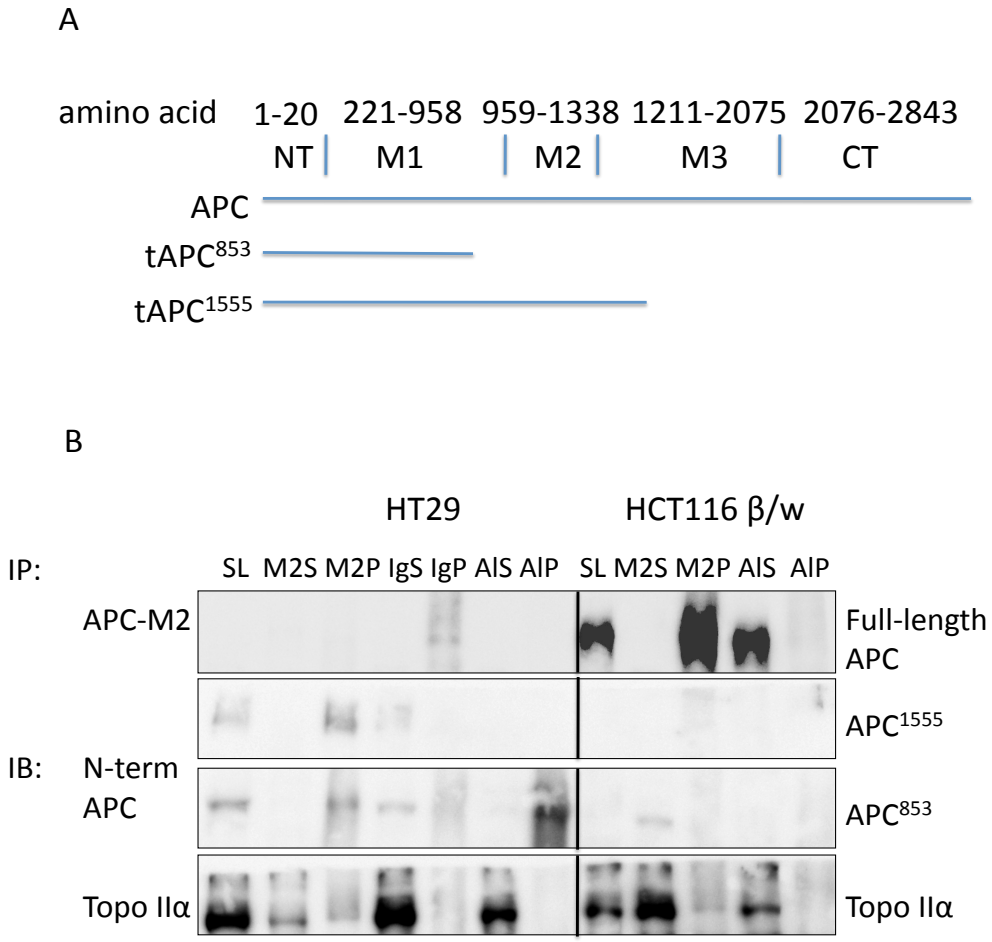

Appendix figure 1.1. t*APC*^{1555} *co-precipitates with topo IIα while tAPC*^{853} *does not.* (A) Diagram of truncated APC in HT29 cells with one allele that is 853 amino acids in length and the second allele on bottom that is 1555 amino acids in length. Along the top are the different APC constructs including NT (amino acid 1-20), M1 (amino acid 221-958), M2 (amino acid 959-1338), M3 (amino acid 1211-2075), and CT (amino acid 2076-2843). (B) Co-immunoprecipitation of both truncated APC proteins endogenous to HT29 cells, tAPC^{853} and tAPC^{1555}, with topo IIα. tAPC^{1555} was precipitated from the soluble lysate (SL) using an antibody specific for the M2 portion of APC (M2-APC). This immunoprecipitation (IP) is labeled as M2S (M2 supernatant) and M2P (M2 pull-down) on the blot. This IP was followed by a second immunoprecipitation of tAPC^{853} from the M2S lysate with an antibody, ALI12-28, specific for the N-terminal portion of APC (labeled ALS for supernatant and ALP for pull-down). IgG IP was used as a control. M2 IP with M2-APC shows that both truncated APC proteins precipitate as well as topo IIα. IP with ALI12-28 shows that tAPC^{853} precipitates but topo IIα does not. HCT116β/w cells were used as a control reaction and show that M2-APC antibody can precipitate full-length APC and topo IIα.

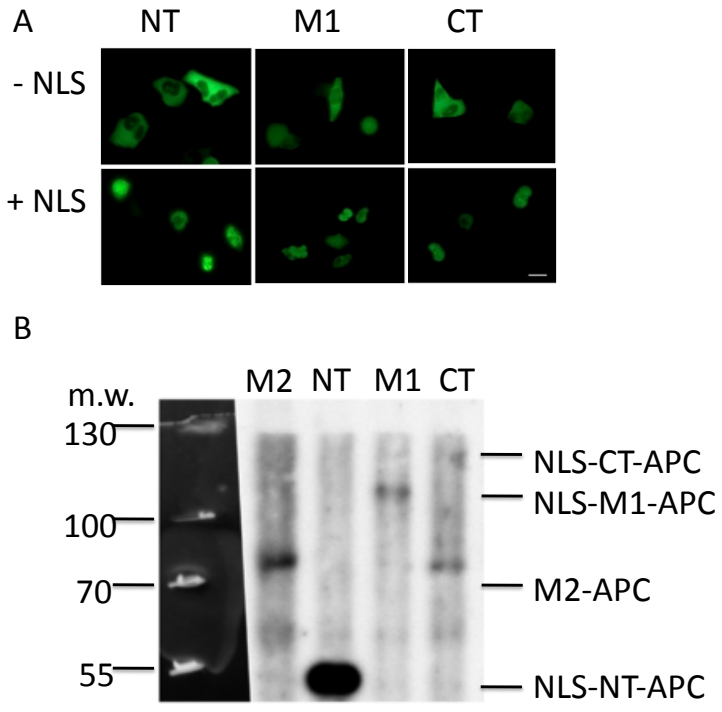
A
NT
M1
CT
- NLS
+ NLS
B
m.w.
M2
NT
M1
CT
130
100
70
55
NLS-CT-APC
NLS-M1-APC
M2-APC
NLS-NT-APC
C
IP:
GFP
M2
APC-M2
- APC
IB:
Topo IIα
GFP
- M2-GFP
- GFP

Appendix figure 1.2. ***NLS fusions facilitated nuclear localization of APC domains, however coimmunoprecipitation of constructs was unsuccessful.*** **(A) The NLS from SV40 large T antigen was cloned upstream of NT-APC, M1-APC, and CT-APC and fusions were expressed in HCT116 β/w cells. Live images were acquired at 400x. Scale bar = 50 μm. (B) Immunoblot showing that all APC domains were immunoprecipitated from HCT116 β/w using a GFP antibody. (C) Cells transfected with M2-GFP construct (positive control) and GFP alone (negative control) show topo IIα in both positive and negative control. Full-length APC was also present in both positive and negative control. HCT116 β/w cells were transfected with each construct and protein was harvested 48 hours after transfection. Immunoprecipitation was performed with a GFP antibody and blots were probed for full-length APC using APC-M2 antibody, for topo IIα, and for M2-APC-GFP and GFP using a GFP antibody.**

Appendix Table 1

Methods used to try to alleviate non-specific binding
1. Invitrogen IP protocol
2. LiCl wash for beads
3. Blocking antibody and beads
4. Multiple GFP antibodies
5. Pre-clear the lysate
6. Removal of potential DNA contamination via manual shredding and DNase

References

1. Murphy, K. J., Nielson, K. R., and Albertine, K. H. (2001) Defining a molecularly normal colon, *J Histochem Cytochem 49*, 667-668.
2. Deweese, J. E., and Osheroff, N. (2009) The DNA cleavage reaction of topoisomerase II: wolf in sheep's clothing, *Nucleic Acids Res 37*, 738-748.
3. Downes, C. S., Clarke, D. J., Mullinger, A. M., Gimenez-Abian, J. F., Creighton, A. M., and Johnson, R. T. (1994) A topoisomerase II-dependent G2 cycle checkpoint in mammalian cells, *Nature 372*, 467-470.
4. Heinen, C. D., Goss, K. H., Cornelius, J. R., Babcock, G. F., Knudsen, E. S., Kowalik, T., and Groden, J. (2002) The APC tumor suppressor controls entry into S-phase through its ability to regulate the cyclin D/RB pathway, *Gastroenterology 123*, 751-763.
5. Jaiswal, A. S., and Narayan, S. (2004) Zinc stabilizes adenomatous polyposis coli (APC) protein levels and induces cell cycle arrest in colon cancer cells, *J Cell Biochem 93*, 345-357.
6. Wang, Y., Azuma, Y., Moore, D., Osheroff, N., and Neufeld, K. L. (2008) Interaction between tumor suppressor adenomatous polyposis coli and topoisomerase IIalpha: implication for the G2/M transition, *Mol Biol Cell 19*, 4076-4085.
7. Wang, Y., Coffey, R. J., Osheroff, N., and Neufeld, K. L. (2010) Topoisomerase IIalpha binding domains of adenomatous polyposis coli influence cell cycle progression and aneuploidy, *PLoS One 5*, e9994.
8. Watanabe, T., Wang, S., Noritake, J., Sato, K., Fukata, M., Takefuji, M., Nakagawa, M., Izumi, N., Akiyama, T., and Kaibuchi, K. (2004) Interaction with IQGAP1 links APC to Rac1, Cdc42, and actin filaments during cell polarization and migration, *Dev Cell 7*, 871-883.
9. Chen, A. Y., and Liu, L. F. (1994) DNA topoisomerases: essential enzymes and lethal targets, *Annu Rev Pharmacol Toxicol 34*, 191-218.